Sensors & Diagnostics

CRITICAL REVIEW

View Article Online
View Journal | View Issue

Cite this: *Sens. Diagn.*, 2026, **5**, 455

Comparative performance of graphene and MXenes in flexible pressure sensors

Mohammed Nabeel, *[a] Nabil Kadhim Taieh,[b] Mohammed Ahmed Shehab, [c] Ying Li, [d] Guangjun Gou,[e] Adnan A. AbdulRazak [f] and Khalid T. Rashid[f]

Two-dimensional nano-conductors have led to the rapid development of flexible pressure sensors; however, studies need to establish direct application-based evaluations between MXene and graphene platforms. Specifically, this review synthesizes recent progress across sensing mechanisms (piezoresistive, capacitive, piezoelectric, and triboelectric), device architectures (microstructured films, porous foams/aerogels, textiles, and hybrid stacks), and performance metrics relevant to wearables and soft robotics. In particular, the operating regime determines the material selection process because graphene crack-network films demonstrate exceptional sensitivity to sub-kPa pressures for micro-physiological pressure measurement but MXene composites and textiles maintain their linear behavior and structural stability during mid- to high-pressure applications with excellent durability. Furthermore, practical limits differ: MXene requires encapsulation to mitigate oxidation and long-term drift in humid or sweat-rich environments, while graphene's crack-mediated transduction can introduce hysteresis and baseline evolution over extended cycling. Finally, the last part introduces a decision framework which links application restrictions to mechanism–material pairings while demanding standardized reporting methods that must include sensitivity ranges and load protocols and hysteresis and durability statistics to improve comparison and translation capabilities. Therefore, these guidelines enable the rational selection and engineering of MXene/graphene sensors for health monitoring and human–machine interfaces and soft robotic touch applications.

Received 12th December 2025,
Accepted 15th January 2026

DOI: 10.1039/d5sd00223k

rsc.li/sensors

1. Introduction

The development of wearable health monitors and soft robotic touch and human–machine interfaces, such as wrist-pulse patches, smart plantar-pressure insoles, prosthetic liners, and soft robotic gripper skins, depends on flexible and stretchable pressure sensors (Fig. 1).[1–5] 2D conductors MXenes and graphene demonstrate exceptional mechanical

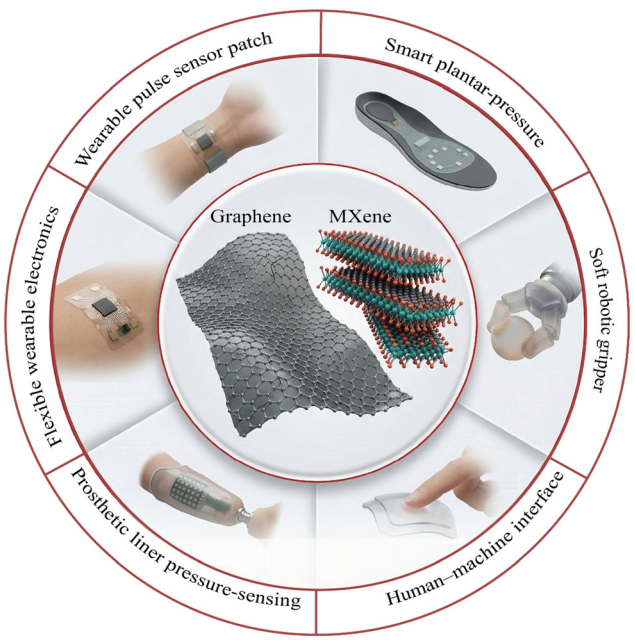

Fig. 1 Representative applications of MXenes and graphene in flexible pressure-sensor technologies.

[a] *Center of Industrial Applications and Materials Technology, Scientific Research Commission, Baghdad, Iraq. E-mail: mohammed.n.ibrahim@src.edu.iq, mohamedxl2006@gmail.com*
[b] *Department of Materials Engineering, Ministry of Higher Education, Middle Technical University, Technical Engineering College Baghdad, Baghdad, 10074, Iraq. E-mail: nabeel_khadum@mtu.edu.iq*
[c] *Gas Processes and Petrochemicals Engineering Department, Basrah University for Oil and Gas, 61004 Basrah, Iraq. E-mail: mohammed.ahmed@buog.edu.iq*
[d] *School of Mechanical Engineering, Chengdu University, 2025 Chengluo Avenue, Chengdu 610106, China. E-mail: liying@cdu.edu.cn*
[e] *School of Materials and Chemistry, Southwest University of Science and Technology, Mianyang, Sichuan, China. E-mail: guangjungou@swust.edu.cn*
[f] *Membrane Technology Research Unit, College of Chemical Engineering, University of Technology-Iraq, Al Sinaa Street 52, 10066 Baghdad, Iraq. E-mail: Adnan.a.alsalim@uotechnology.edu.iq, Khalid.t.rashid@uotechnology.edu.iq*

compliance and high conductivity and suitable integration with thin elastomers and textiles and porous scaffolds.[6,7] However, real device architectures reveal different performance characteristics of these materials despite their initial advantages.[8] For example, the detection of tiny loads becomes possible through graphene when it is used in ultrathin films that utilize controlled crack/tunneling pathways.[9] MXenes maintain a wide range of quasi-linear behavior when integrated into foams and aerogels and textile networks because they demonstrate excellent resistance to high compression and multiple loading cycles.[10] The observed differences between these materials reach beyond basic material characteristics.[11] The tests establish whether a device can detect wrist pulses without interference and measure plantar loads through an insole and withstand robotic gripper operational cycles.[12]

A central theme of this review is that the microstructure and architecture govern performance as much as intrinsic chemistry. The nanoscale junctions in crack-engineered graphene films provide them with exceptional sensitivity to detect low pressure values.[9] In parallel, MXene networks embedded in compressible scaffolds develop additional contact points during loading operations while preserving their resistance to saturation, which enables them to function across

Mohammad Nabeel

Mohammad Nabeel received his Ph.D. in Materials Science and Technology and is a graduate of the University of Miskolc, Hungary (2024). He is currently affiliated with the Scientific Research Commission, Iraq. His research interests focus on flexible and wearable sensors, electronic skin (e-skin), and nanocomposite pressure sensors based on nanomaterials such as MXenes, graphene and carbon nanotubes. His work emphasizes application-driven sensor design, performance reliability, environmental stability, and comparative evaluation of sensing mechanisms for wearable electronics and soft robotic systems. He has authored several peer-reviewed publications in high-impact journals in the field of flexible electronics and advanced functional materials.

Nabil Kadhim Taieh

Nabil Kadhim Taieh is an Associate Professor of Materials Engineering at Middle Technical University, Baghdad, Iraq. He received his Ph.D. in Materials Science and Engineering from Southwest Jiaotong University, China, in 2021. His research focuses on polymer and fiber-reinforced composites, graphene-based aerogels, multifunctional sandwich structures, and microwave absorption materials. His work also covers corrosion protection, surface engineering, and advanced material characterization. He has authored numerous peer-reviewed publications in international journals and serves as a reviewer for several high-impact journals in materials science and engineering.

Mohammed Ahmed Shehab

Mohammed Ahmed Shehab received his B.Sc. and M.Sc. degrees in Chemical Engineering from the University of Technology/Baghdad in 2008 and 2015, respectively. In 2024, he earned his Ph.D. in Chemical Engineering from the University of Miskolc, Hungary. Since 2016, he has been serving as a lecturer at Basrah University for Oil and Gas.

Ying Li

Li Ying is an Associate Professor and obtained her PhD in Materials Science and Engineering from Southwest Jiaotong University in 2020. She is currently a specially-appointed researcher and master's supervisor at Chengdu University. Her primary research interests include electromagnetic protective materials, thermal conductive composites, energy materials, and material simulation and computation. She has published multiple research papers in international academic journals such as Chemical Engineering Journal, ACS Applied Materials Interfaces, and Carbon, and holds several authorized patents. She serves as a reviewer for several international academic journals, including Nature Communications, Journal of Advanced Ceramics, and Small.

a broader range.[13] Moreover, the combination of 2D sheets with 1D nanowires through hybrid methods produces networks which show better stability and prevent restacking and exhibit improved resistance to bending and compression.[14]

Besides these mechanisms, the advantages of machine translation require evaluation against operational barriers which impact translation operations.[15] Specifically, MXenes (*e.g.*, $Ti_3C_2T_x$) show chemical sensitivity because they undergo oxidation reactions with oxygen and moisture, which cause electrical resistance growth and material drift until they receive protective encapsulation or matrix materials.[16] By comparison, the chemical stability of graphene films exists but their mechanical strength deteriorates when subjected to high strain levels. As a result, the microcracks that generate ultrahigh sensitivity in sensors expand or transform during cycling operations, which results in hysteresis effects and baseline movement.[17] Consequently, the reproducibility of both families becomes difficult because stochastic percolation or crack networks produce different results between devices when manufacturing processes do not have strict control.[15]

Accordingly, we emphasize standardized descriptors (*e.g.*, $\Delta R/R_0$ kPa^{-1} or $\Delta C/C_0$ kPa^{-1} over specified pressure windows), clear load protocols with loading/unloading curves and hysteresis, and durability statistics across cycles and devices.[15,17] Such standardized reporting is essential to enable meaningful cross-study comparisons and to avoid misleading performance claims based on selective pressure windows. In turn, basic reporting requirements would stop selective data presentation which would result in reliable results for assessing group performance.[15]

Unlike previous reviews that focus exclusively on either graphene- or MXene-based pressure sensors, this work provides a direct, application-driven comparison between the two material platforms across identical sensing mechanisms (piezoresistive, capacitive, piezoelectric, and triboelectric) and device architectures. Rather than listing performance metrics in isolation, we explicitly map the pressure regime (sub-kPa, mid-range, and high-load operation), signal type (static *vs.* dynamic), and durability requirements to material–mechanism combinations. Furthermore, we consolidate detection limits (LODs), sensitivity windows, hysteresis behavior, and cycling endurance into a unified decision framework aimed at guiding material selection for wearable and soft robotic applications. This comparative and decision-oriented perspective distinguishes the present review from prior graphene- or MXene-focused surveys.

2. Materials science basis of MXenes and graphene

2.1 MXene fundamentals (structure, chemistry, and stability)

MXenes form from $M_{n+1}AX_n$ (MAX) phases through A-layer (Al) etching to produce 2D carbide/nitride sheets which have nanometer-scale thickness and surface terminations of –O, –OH, and –F (Fig. 2a–c).[18–20] MXenes become hydrophilic through these termination processes, which allows them to disperse in water and polar solvents for applications in printable inks and spray coatings and polymer integration.[21] The material $Ti_3C_2T_x$ shows metallic-like conductivity because researchers have measured conductivities between 10^4–10^5 S m^{-1} in the film form and 4.6×10^5 S m^{-1} in single-sheet measurements.[22] Such high conductivity allows MXene-based networks to transduce pressure-induced contact changes with low joule loss, which is attractive for stable, low-power sensing.[23,24] However, the main drawback is that the environment remains unstable. Specifically, the oxidation of Ti-based MXenes occurs when they are exposed to air and humidity, which results in the formation of TiO_x and a decrease in their electrical conductivity (Fig. 2d).[25] Moreover, the degradation process of these materials becomes significant when they are exposed to sweat and air for weeks to months without protective measures such as encapsulation

Guangjun Gou

Guangjun Gou is a Lecturer at the Southwest University of Science and Technology, China. His research interests focus on biomass-derived materials, functional composites, and oil-field chemical materials, with particular emphasis on porous carbon materials and their applications in electromagnetic wave absorption. His work involves the design and synthesis of advanced carbon-based and hybrid functional materials, as well as interfacial engineering for performance optimization. He has authored multiple peer-reviewed publications and actively contributes to research in functional materials and energy-related applications.

Adnan A. Abdulrazak

Adnan A. Abdulrazak is a Professor of Chemical Engineering at the University of Technology, Iraq. He received his Ph.D., M.Sc., and B.Sc. degrees in Chemical Engineering from the University of Technology. His research interests include nanotechnology, composite materials, membrane technology, environmental and refinery engineering, and sustainable chemical processes. He has held academic positions ranging from Lecturer to Professor and served as a Visiting Professor at Western University, Canada. He has published extensively in peer-reviewed journals and supervised numerous postgraduate theses in chemical and materials engineering.

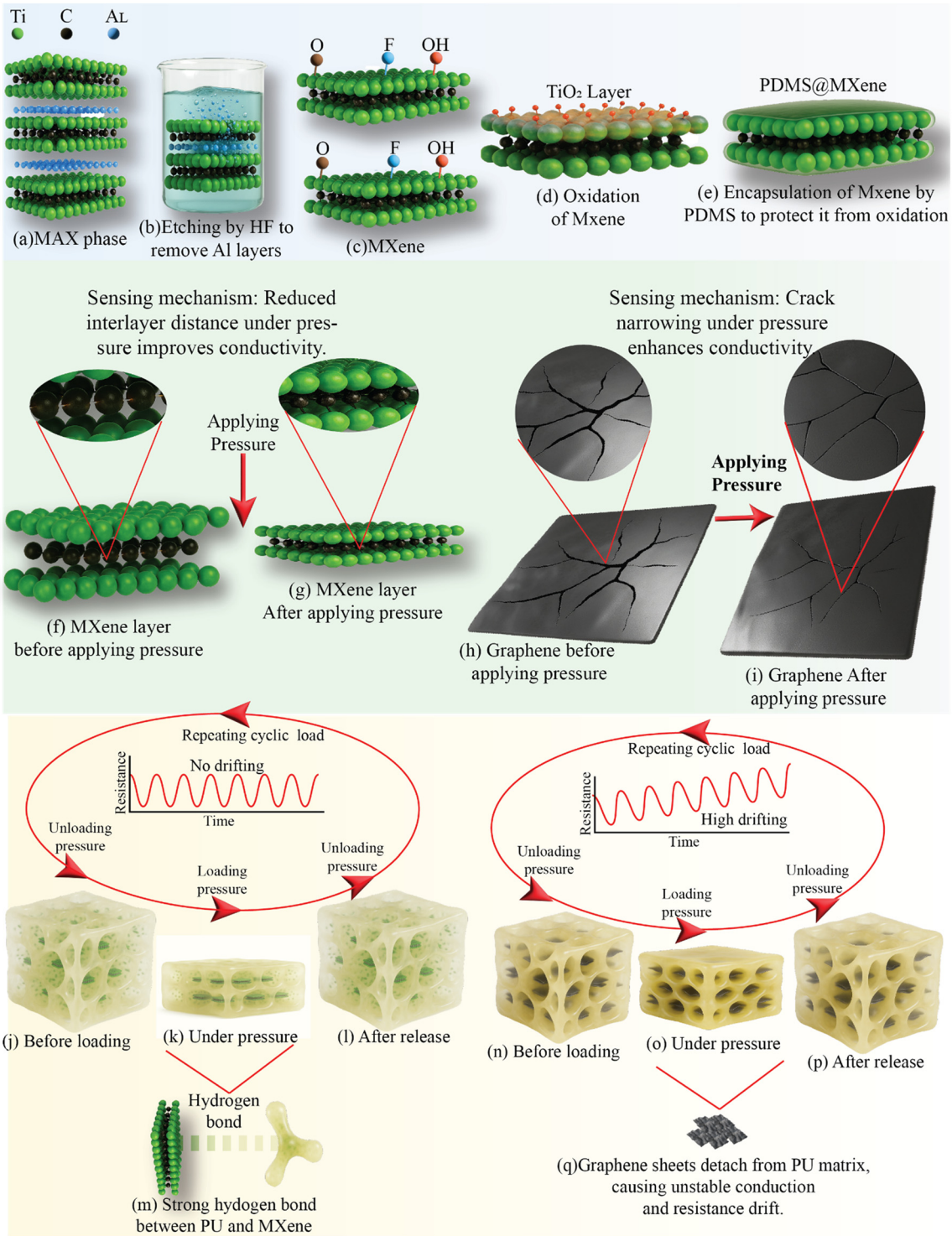

Fig. 2 Comparative mechanisms of MXene- and graphene-based pressure sensors and their cyclic stability within polymeric matrices. The figure illustrates the synthesis and surface chemistry of MXene from MAX phases, including HF etching and surface terminations (–O, –OH, –F) (a–c), followed by oxidation-induced degradation and encapsulation with PDMS for environmental protection (d and e). The pressure sensing mechanism in MXene relies on reduced interlayer spacing and enhanced interflake contacts under compression, leading to increased conductivity (f and g). In contrast, graphene-based sensors operate through crack-narrowing and tunneling-dominated conduction, where applied pressure closes microcracks and decreases resistance (h and i). Cyclic compression of MXene–PU composites exhibits stable resistance with minimal drift due to strong interfacial hydrogen bonding and reversible scaffold deformation (j–m). By comparison, graphene–PU composites show higher resistance drift and poor recovery under repeated loading, attributed to weak interfacial adhesion and progressive detachment of graphene sheets from the polymer matrix (n–q).

polyurethane (PU) and polydimethylsiloxane (PDMS) (Fig. 2e) or antioxidant treatments.[16] Nevertheless, devices operate through interlayer sliding in stacked or composite structures.[26,27] MXene flakes in pristine multilayer films experience cracking and delamination when subjected to strain because of the van der Waals forces between them.[28] However, MXene flakes achieve improved toughness and flexibility when embedded in polymers such as PU and polyvinyl alcohol (PVA) to create composites which withstand extreme bending and compressive forces before breaking.[29,30] In addition, the internal structure of porous scaffolds (PU foams and aerogels) becomes covered by MXene which creates a three-dimensional network of conductive pathways.[13] The interflake distance decreases and conductive contacts increase when compressed, which produces a mostly linear piezoresistive response across extensive pressure ranges while maintaining electrical conduction above 50% compressive strain (Fig. 2f).[13] MXene-coated sponges show resistance to 10^3–10^4 compression cycles and maintain stable resistance during each cycle.[13,31] Overall, MXenes possess outstanding electrical properties and processing capabilities for foam and composite materials yet need protection against oxidation and encapsulation by for example PDMS to ensure their long-term functionality (Fig. 2e).[32]

2.2 Graphene fundamentals (forms and sensing behavior)

Graphene is a one-atom-thick sp^2 carbon sheet with very high carrier mobility and excellent in-plane conductivity ($\sim 10^4$–10^5 S cm^{-1} for high-quality material).[33] The literature reports four primary methods to implement graphene in flexible pressure sensors through (i) chemical vapor deposition (CVD) graphene film transfer onto elastic materials and thin plastic substrates.[34] (ii) Printing graphene flakes or reduced graphene oxide (rGO) to create conductive paths through junctions.[35] (iii) 3D graphene foam production starts with metal foam templating during CVD followed by etching steps. (iv) Solution-based GO/rGO films allow mass production through deposition techniques.[36,37] These morphologies create layers that can be applied to flexible materials which include fabrics and microstructured elastic materials. Moreover, a defining sensing mechanism in many graphene-based pressure sensors is the microcrack- or tunneling-dominated piezoresistive response. The natural development of nanoscale cracks and partial separation happens in ultra-thin graphene films and graphene/rGO coatings which are applied to elastomers.[9] The current flows through a small number of fragile junctions (high resistance).[38] The resistance shows a substantial decrease when the local contact area expands and tunneling gaps decrease in size under typical pressure conditions (Fig. 2h and i). This yields extremely high sensitivity in the sub-kPa regime. For example, the reported sensors achieve sensitivity levels of 10^4–10^5 kPa^{-1} when operating at pressures below 0.5 kPa and optimized microstructured graphene films achieve pressure detection at the Pa level.[39] As a result, this behavior is ideal for applications such as pulse monitoring, vocal/throat sensing, facial micro-movement mapping and light-touch tactile interfaces.[39] However, the same mechanism that creates cracks in the material structure leads to performance limitations.[17] The sensitivity of most cracks to pressure changes becomes minimal after they close at a pressure of a few kPa.[40] Furthermore, the repeated cycling process causes cracks to spread which results in hysteresis effects between loading and unloading curves and baseline resistance drifts that occur throughout time (Fig. 2n–q). Graphene foams and elastomer composites filled with graphene show different compression behavior because they compress like sponges while their conductive paths become denser.[41] As such, the structures show high compressive strain values above 40–50% when operating at broad pressure ranges yet they exhibit lower sensitivity than ultrathin crack-engineered films.[39,42] Overall, the ultra-low-pressure sensitivity of graphene reaches exceptional levels while its detection limits become extremely low but this performance comes with restricted linear range operation and increased hysteresis and potential long-term crack formation issues.[43,44]

2.3 Microstructure–mechanics link in composite sensors

MXenes and graphene exist in most practical devices as individual components which are embedded inside soft structured matrices that include PDMS, Ecoflex, PU foam, thermoplastic polyurethane (TPU), hydrogel and textile materials.[6] Accordingly, the electromechanical response is then governed by how the conductive network evolves under compression.[45] In percolating composites, pressure reduces interparticle distance, increases contact area and/or opens new conduction pathways, decreasing resistance in a largely monotonic, piezoresistive way.[46] MXene polymer composites achieve their enhanced performance through the MXene's sheet-like structure and surface terminations, which enable close polymer contact and sustained interflake connections under cyclic loading conditions (Fig. 2j–m).[47] MXene networks based on foam or aerogel materials exhibit wide operational pressure ranges and minimal hysteresis because they form additional contact points when subjected to increased pressure.[48] By contrast, the failure behavior of graphene-based composites follows the same percolation principles as other composites but shows unique failure patterns. The tunneling barriers between flakes in rGO networks experience major changes when subjected to small compressions. This led to producing high sensitivity at low loads, but leads to permanent network rearrangement and drift.[15] In addition, the dome tips of microstructured arrays create adjustable contact areas with elastomer surfaces, which enables the formation of conductive junctions that decrease resistance speedily based on applied pressure.[46] Sensitivity is extremely high at first contact, and then levels off as full contact is reached. Meanwhile, MXene or graphene-coated porous foams function as compressible scaffolds because their cell walls compress in a stepwise manner under load, which generates linear stress–strain behavior up to tens of kPa while preserving functionality during thousands of

loading cycles.[49] Moreover, interfacial chemistry serves as a vital factor in this process. For example, MXene functional groups establish hydrogen bonding and other chemical interactions with polymers, which enables the network to reset after unloading and decreases hysteresis.[50,51] Conversely, the chemical inertness of pristine graphene along with its ability to slide between interfaces results in increased hysteresis unless it receives modifications through functionalization or polymer coating or secondary nanofiller hybridization.[52,53] The combination of 2D sheet structures with 1D nanowires (*e.g.* graphene + CNTs and MXene + Ag nanowires) creates a hybrid system that provides better connectivity and prevents restacking and achieves superior mechanical strength against bending and compressive forces.[54] Overall, the performance of sensors relies on microstructure instead of sheet properties because graphene needs crack networks for ultrahigh sensitivity at small loads and MXene-based foams/composites achieve a wide pressure range and cycling stability through their percolating conductive scaffolds. MXene enhances conductivity through reduced interlayer spacing, while graphene enhances conductivity via crack narrowing under applied pressure (Fig. 2f–i). The MXene–PU composite shows reversible deformation and stable resistance during cyclic loading due to strong interfacial hydrogen bonding (Fig. 2j–m), while the graphene–PU composite exhibits higher resistance drift and poor recovery because of weak interfacial adhesion (Fig. 2n–q).

2.4 Mechanical compliance and durability of MXene and graphene sensors

Both MXene- and graphene-based pressure sensors are designed to be mechanically compliant, typically on thin elastomeric or plastic substrates that can bend to millimeter-scale radii without significant signal loss.[55] Graphene films on polyethylene terephthalate (PET), for example, remain functional when wrapped around ~5 mm radius surfaces. Similarly, MXene-coated textiles and thin MXene films maintain stable resistance under repeated bending to ~3 mm radius or 90° flexing.[55] Pure, continuous MXene or graphene films are not intrinsically stretchable—they tend to crack under large tensile strain—so stretchability is usually achieved by structural engineering: patterning serpentine traces, embedding flakes in elastomers, or producing fiber and foam architectures. Graphene–rubber composites can tolerate >20% tensile strain as functional sensors, and MXenes integrated into stretchable polymer fibers have been reported to sustain >100% strain without electrical failure.[56,57] While many pressure sensors mainly experience compression rather than tensile stretching in use, bendability is essentially mandatory for wearables and e-skin. Durability under cyclic loading is another key differentiator. MXene-based composites and aerogels often show highly repeatable piezoresistive behavior over thousands to tens of thousands of compression cycles (*e.g.* stability reported beyond 10^3–10^4 cycles, and in some cases ~25 000 cycles).[58] This resilience is attributed to MXene flakes forming robust, contact-rich networks within elastic scaffolds, which absorb compression without severe fracture or delamination. Graphene sensors can also be durable, but their dominant mechanism—pressure-driven closing/reopening of microcracks and tunneling gaps—can introduce hysteresis and early-cycle drift. Many graphene crack-network sensors exhibit an initial "training" period in the first ~10^2 cycles where cracks stabilize, followed by relatively stable output over >10^3 cycles, though some baseline drift typically remains. By contrast, when MXene or graphene serves primarily as a flexible electrode in capacitive or piezoelectric devices, rather than as the active piezoresistive network, cycling endurance can exceed 10^5 load cycles because the sensing no longer depends on repeatedly breaking/reforming conduction pathways.[59–61] Under high-pressure or high-strain compression, MXene-infused foams and aerogels generally retain structural integrity and electrical continuity even at >50% compressive strain and at pressures extending to >100 kPa, in some reports up to the 100–150 kPa range and beyond.[62,63] Certain MXene–textile systems have even tolerated loads approaching the MPa level without catastrophic failure.[63] Graphene can achieve comparable wide-range robustness when configured as a 3D foam or laser-scribed graphene sponge, which distributes stress through a porous, recoverable network and enables sensing up to tens of kPa (*e.g.* ~50 kPa) without immediate saturation.[64] However, ultra-thin planar graphene films on flat substrates are more vulnerable: excessive normal force can permanently propagate cracks or collapse the percolation network unless the film is pre-patterned or supported by a microstructured elastomer.

In summary, both MXenes and graphene can deliver flexible, bendable, and even stretchable pressure sensors with multi-thousand-cycle endurance. Graphene excels in ultrahigh sensitivity at low pressure but can suffer from crack-driven hysteresis and drift under cycling. MXene composites excel in mechanical robustness under repeated compression and in a broad pressure range but face long-term chemical stability concerns (oxidation and embrittlement) in humid, skin-contact environments.

3. Sensing mechanisms in flexible pressure sensors

Flexible pressure sensors operate through four main mechanisms which include piezoresistive, capacitive, piezoelectric and triboelectric. Here, we focus on how MXene- and graphene-based devices operate under each mechanism, and how the same material can act either as the active sensing network (changing resistance with pressure) or as a compliant electrode.

3.1 Piezoresistive sensing

Piezoresistive sensing relies on pressure-induced changes in electrical resistance: when an external load compresses a conductive network, the geometry of that network and the number/quality of conductive contacts changes, which modifies the measured resistance (Fig. 3a).[65] For example, MXene sheets (*e.g.* $Ti_3C_2T_x$) can form a percolating conductive network in a compressible scaffold such as a

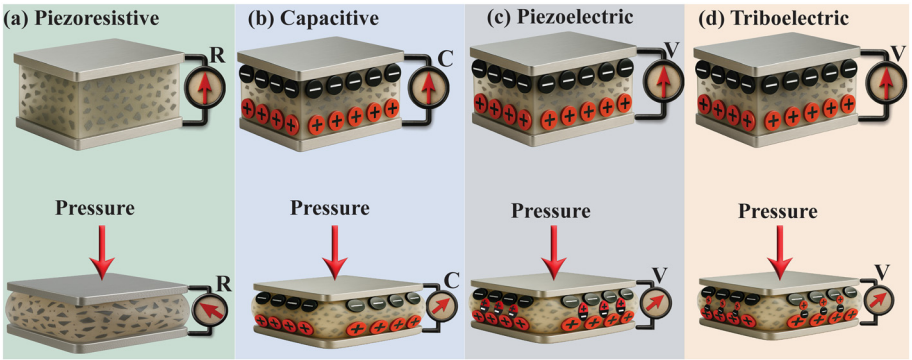

Fig. 3 Sensing mechanisms in flexible pressure sensors (a) piezoresistive, (b) capacitive, (c) piezoelectric and (d) triboelectric.

coated foam or an elastomeric composite.[65] At zero load, baseline resistance is dominated by the largest inter-sheet gaps; when pressure is applied, the structure compresses, MXene sheets move closer, new contact points form, the contact resistance associated with those gaps (R_c) drops, and total resistance decreases.[65] As a result, MXene-based foams and aerogels exhibit a mostly linear resistance change across a wide pressure range because their compression process creates multiple parallel conduction paths that become denser instead of depending on a single fracture point. For instance, MXene aerogel/foam sensors achieve sensitivity values of ~331 kPa^{-1} in the 0–0.5 kPa range and ~126 kPa^{-1} in the 0.5–7.5 kPa range while maintaining functionality at pressures above 7 kPa. Similarly, the sensitivity of other MXene/foam designs remains linear from 0 to 100 kPa with sensitivity values ranging between ~1 and 5 kPa^{-1}. Moreover, the stability of cycling remains strong because MXene shows less than 5% drift after 10 000 cycles when it is properly attached to an elastic scaffold.[65–67] However, MXene requires encapsulation or antioxidant treatment to protect its conductivity from degradation when exposed to humid or sweat-rich environments because it oxidizes under such conditions which leads to conductivity changes and long-term drift.[68]

The piezoresistive sensing mechanism of graphene-based sensors depends on the occurrence of microcracks and tunneling effects. Specifically, the combination of graphene films with stretchable substrates leads to nanoscale defects that recover partially through minor pressure changes, which produces a major reduction in resistance. Consequently, the method produces high sensitivity to minimal pressure changes because results show ~232.5 kPa^{-1} sensitivity in 0–0.2 kPa through controlled microcrack engineering in wearable graphene sensors which detect throat-vibration-level pressures.[64,69] Alternatively, graphene can also be integrated as a conductive sponge or composite (graphene or rGO dispersed in PU foam/elastomer), which gives more moderate sensitivities (~0.79 kPa^{-1} with ~75 Pa detection limit and >10 000 stable cycles,[55] or ~0.1–1 kPa^{-1} over 0–20 kPa in graphene foams) and a broad usable range.[64,70] However, the two main engineering problems that occur are (i) hysteresis: the loading and unloading curves do not overlap because cracks open and relax differently with ~10–20% hysteresis observed at higher pressures, and (ii) the crack network undergoes structural changes during repeated cycling, which causes the baseline to shift over time.[65] To mitigate this, the introduction of microstructured supports (wrinkles and microdomes) under graphene films enables strain distribution which slows down crack growth and enables operation at elevated pressures before material failure occurs.

In summary, the two piezoresistive sensing methods use MXene networks and graphene-based crack/tunneling films to detect pressure through distinct physical mechanisms where MXene densifies its 3D conductive structure and graphene adjusts its nanoscale crack junctions. Accordingly, the various synthesis methods result in different operational requirements because MXene needs oxidation control and graphene requires hysteresis and drift management.

3.2 Capacitive sensing

Capacitive pressure sensing measures changes in capacitance between two electrodes separated by a compressible dielectric layer: applying pressure reduces the gap (or changes the dielectric geometry/permittivity), which increases capacitance (Fig. 3b).[71] In such devices, MXene or graphene in flexible capacitive sensors functions as a thin flexible electrode instead of a dielectric material.[72] MXene/AgNW electrode capacitive sensors with PDMS dielectrics achieve pressure detection sensitivity down to 16 mg during their operation within the 0 to 600 kPa range. Vertical graphene (VG) electrodes with microstructured dielectrics demonstrate two distinct sensitivity ranges which amount to 6.04 kPa^{-1} for 0–1 kPa and 0.69 kPa^{-1} for 1–10 kPa. Additionally, the combination of Ag nanowires and CNTs in 1D electrode structures prevents MXene sheet stacking while enabling stretchability and maintaining stable contact resistance during multiple loading cycles.[72,73] Notably, the MXene/AgNW-electrode capacitive sensors with patterned PDMS dielectrics achieve pressure detection sensitivity of 10.13 MPa^{-1} in the 0–100 kPa range while detecting pressure changes below 16 mg across 0 to 600 kPa.[73]

The quasi-static readout of capacitive sensors enables their use in wearable technology, while their low hysteresis and minimal power consumption through small AC sensing make them suitable for continuous monitoring.[71] The combination of micro-domes and interlocked/porous dielectrics in sensors generates increased local strain which results in enhanced detection of small pressure variations. The VG-electrode capacitive sensors demonstrated a sensitivity of 6.04 kPa^{-1} when operating within the pressure range of 0–1 kPa.[73] However, the system faces two main limitations which include environmental sensitivity to humidity and nearby objects that can affect fringe fields and dielectric saturation when the material reaches its maximum collapsed state.[74] The range of these devices can be extended by using multilayer or porous dielectrics and textile/air-gap spacers. For example, a MXene–textile capacitive device with a porous fabric dielectric showed a near-linear response up to 1.5 MPa.

MXenes and graphene function as flexible high-conductivity electrodes in capacitive stacks according to the materials analysis. In particular, MXenes offer very low sheet resistance at small thickness but are moisture-sensitive, while graphene- or VG-based electrodes are chemically robust and printable/transferable, although achieving equally low sheet resistance may require thicker coatings. Consequently, the materials function as capacitive sensors to monitor pressure distribution for respiration and posture and plantar load analysis with high repeatability and minimal drift and sub-Pa detection sensitivity.

3.3 Piezoelectric sensing

Piezoelectric pressure sensors produce electrical signals through changes in piezoelectric material polarization when mechanical stress occurs; these sensors detect dynamic events like force onset and offset and vibrations instead of steady loads (Fig. 3c).[75] Accordingly, polyvinylidene fluoride (PVDF) and PVDF-trifluoroethylene (TrFE) films and fibers serve as piezoelectric materials in flexible piezoelectric systems which use MXenes or graphene as conductive additives to boost mechanical strength and electrical charge collection. For example, the addition of a tiny amount of graphene to PVDF results in a major increase of the effective piezoelectric coefficient d_{33} from ~22 pC/N to ~39.7 pC/N at ~0.11 vol% graphene because of better β-phase crystallinity and superior stress transfer.[76] Similarly, electrospun PVDF/MXene fiber mats generate voltage sensitivities of ~0.0048 V N^{-1} because MXene creates an internal conductive path that improves charge collection.[77] In addition, the use of ultrathin MXene or CVD graphene electrodes in place of brittle metal foil enables the creation of flexible and semi-transparent patches which can be applied to skin or textiles to detect arterial pulse waves and throat vibrations.

Notably, piezoelectric sensors typically exhibit very fast response (3.5 ms for thin PVDF films) and can be treated as "self-powered", since they produce a voltage transient without external bias; however, a high-impedance readout circuit is still required.[78] Consequently, the generation of charge through stress changes makes piezoelectric sensors work best with dynamic inputs because static or slowly changing loads cause signals to fade away from charge redistribution.[75] However, the technology has two main limitations because (i) it fails to detect steady constant forces (the signal strength decreases when the material is subjected to static pressure because charges move to new positions) and (ii) piezoelectric polymers need electrical poling to align their dipoles but this process can cause depolarization through heat exposure or mechanical wear.[75] Accordingly, the integration of piezoelectric PVDF/MXene or PVDF/graphene layers with resistive or capacitive layers in stacked configurations allows groups to monitor both dynamic and static information through a single hybrid device.

3.4 Triboelectric sensing

Triboelectric pressure sensors known as triboelectric nanogenerators (TENGs) produce electrical signals through contact and separation of materials with different triboelectric properties (Fig. 3d). The real contact area between materials changes when pressed, which leads to a change in transferred charge and produces an AC voltage/current pulse. TENGs operate similarly to piezoelectric devices because they detect contact changes and impacts instead of static pressure but they produce higher voltage outputs (tens to hundreds of volts) when pressed lightly and function as self-powered devices for touch interfaces and electronic skin applications.[79,80] MXenes and graphene are typically used as compliant electrodes or conductive layers that collect and route charge, and in some cases are patterned directly into the tribo-contact surface to increase available contact area.[79] For example, porous laser-induced graphene (LIG) and vertical graphene walls provide large effective area and have been integrated into triboelectric arrays for spatial touch mapping and machine-learning-based gesture recognition.[81] MXene coatings on textiles or yarns have been used so that pressing a fabric node both generates a triboelectric pulse (sufficient to trigger LEDs) and provides a stable conduction path for extracting the signal. The surface chemistry of graphene can be adjusted to function as either a tribo-positive or tribo-negative material, while its transparent and flexible nature enables the creation of thin tactile pads. MXene shows improved output and extended durability through its high surface charge density and printable hybrid capabilities with Ag nanowires which protect electrodes from damage.[81]

The advantages of triboelectric sensing include self-powered operation and high sensitivity to small dynamic forces such as airflow and tapping and throat vibration and mechanical robustness that depends on surface contact and separation rather than bulk compression. However, a signal becomes transient when a sustained force stops generating current because it exists only briefly. The process of absolute pressure calibration becomes challenging because surface charge dissipation from humidity and sweat leads to sticking behavior which causes measurement consistency to decrease over time. Therefore, the literature studies hybrid stack

systems which combine triboelectric layers based on graphene or MXene electrodes with piezoelectric or resistive/capacitive layers to enable both event detection and force magnitude measurement in wearable human–machine interfaces and soft robotic skins.

3.5 Mechanism–application mapping

The selection of sensing mechanisms between piezoresistive, capacitive, piezoelectric and triboelectric depends on particular application requirements, while MXene and graphene selection determines the final performance level. The two most suitable sensor types for static or slowly changing load applications are piezoresistive and capacitive sensors because they produce dependable output signals when operating under constant pressure conditions.[82] For example, MXene-based piezoresistive foams produce consistent quasi-linear output signals when subjected to various pressure ranges from 0.43–275 kPa which includes both small and large pressure changes. The material shows no signs of degradation during multiple loading cycles at high pressure levels. However, graphene piezoresistive films detect static pressure but their sensitivity decreases because microcracks develop from prolonged loading periods.[49] Meanwhile, MXene and graphene electrodes in capacitive sensors provide excellent performance for continuous static monitoring applications including blood pressure contact sensing and seat occupancy detection because they exhibit minimal hysteresis and electrode impedance stability. The choice between graphene and MXenes depends on specific requirements since graphene works well for thin transparent films but MXenes offer better performance for low impedance electrodes and large area printing applications.[82,83] Additionally, graphene piezoresistive films are needed for wrist pulse and throat vibrations and facial micro-movements because they achieve superior performance at ultra-low pressure levels through engineered crack networks that detect pressure below 1 kPa and track small pressure waves of 0.5 kPa through large resistance changes. PVDF/PVDF-TrFE piezoelectric patches with MXene or graphene-based electrodes convert sub-kPa dynamic oscillations into voltage signals which extract precise time-dependent information from throat vibrations and pulse patterns.[69,84] MXene-based piezoresistive composites (MXene in PU sponge or layered MXene films) work best for wide-range and high-load applications such as robotic touch (0–50 kPa grip) and prosthetic interfaces and plantar pressure mapping in gait (up to hundreds of kPa), because they maintain their sensitivity and linear response across tens to hundreds of kPa and show high durability (often $>10^3$–10^4 cycles). By comparison, graphene foams operate in this pressure range but their operational stability becomes lower when they do not have a polymer support.[49,85] MXene-based piezoresistive fabrics and microstructured capacitive designs used in textile pressure sensors achieve near-MPa to MPa-class ranges for gait and load monitoring applications while showing suitable durability.[83] Accordingly, the use of capacitive sensing becomes suitable for ultra-low-power wireless systems and long-term patches and passive readout nodes because it requires minimal energy for investigation and electrode stability becomes essential in this context. The use of graphene electrodes provides resistance to oxidation but MXene electrodes need encapsulation to stop oxidation degradation because of their high conductivity which enables thin conductive patterns. Self-powered tactile interfaces that include robotic skins and smart gloves require triboelectric and hybrid tribo/piezoelectric sensors as their preferred sensing technology because MXenes and graphene function as flexible electrodes which produce voltage spikes when touched without external bias to detect events and harvest energy, but absolute force calibration remains difficult and sensor output gets affected by humidity levels.[86,87] The analysis shows that graphene-based piezoresistive and piezoelectric sensors work best for detecting ultrasensitive dynamic biosignals at sub-kPa levels. Conversely, MXene-based piezoresistive and MXene-enhanced capacitive systems show better performance for robotics and prosthetics and gait applications that require static or high-load sensing. Therefore, the choice of capacitive sensors made from any material becomes the best option for low-power continuous monitoring applications. Finally, MXene/graphene electrodes in triboelectric/piezoelectric designs show great potential for self-powered touch interface applications.

4. Device architectures and fabrication routes

4.1 Common sensor architectures

The literature shows how MXene integration with graphene depends on specific device architectures which lead to distinct performance outcomes. Accordingly, in this section we describe the physical architectures themselves—how they generate signals and why they can be highly sensitive or wide-range without yet assigning specific applications to each design.

- Microstructured film/sandwich structures: a flat or microstructured dielectric layer is enclosed between two compliant conductive layers; this is widely used in capacitive and some piezoresistive sensors (*e.g.* PDMS between two MXene-coated electrodes, or a thin graphene resistive film encapsulated so that applied pressure compresses it) (Fig. 4a).[34,72] These stacks are pixel-addressable by design because the top and bottom electrodes can be patterned into addressable elements. The middle layer becomes more sensitive when engineers create microdomes or other relief features because the dome tips start with minimal contact which leads to rapid expansion of contact area when pressure increases, thus creating significant resistance or capacitance changes. In this context, active layers in graphene films and MXene films maintain their ultrathin structure which allows them to operate as flexible electrodes in sandwich cells without creating noticeable stiffness.
- Porous foam/aerogel structures: here, the active element is a compressible 3D network rather than a flat film (Fig. 4b). Pressing the network (*e.g.* PU foam coated with MXene or graphene foams/aerogels) changes the overall resistance or contact pathway density through the scaffold.[49,88] The

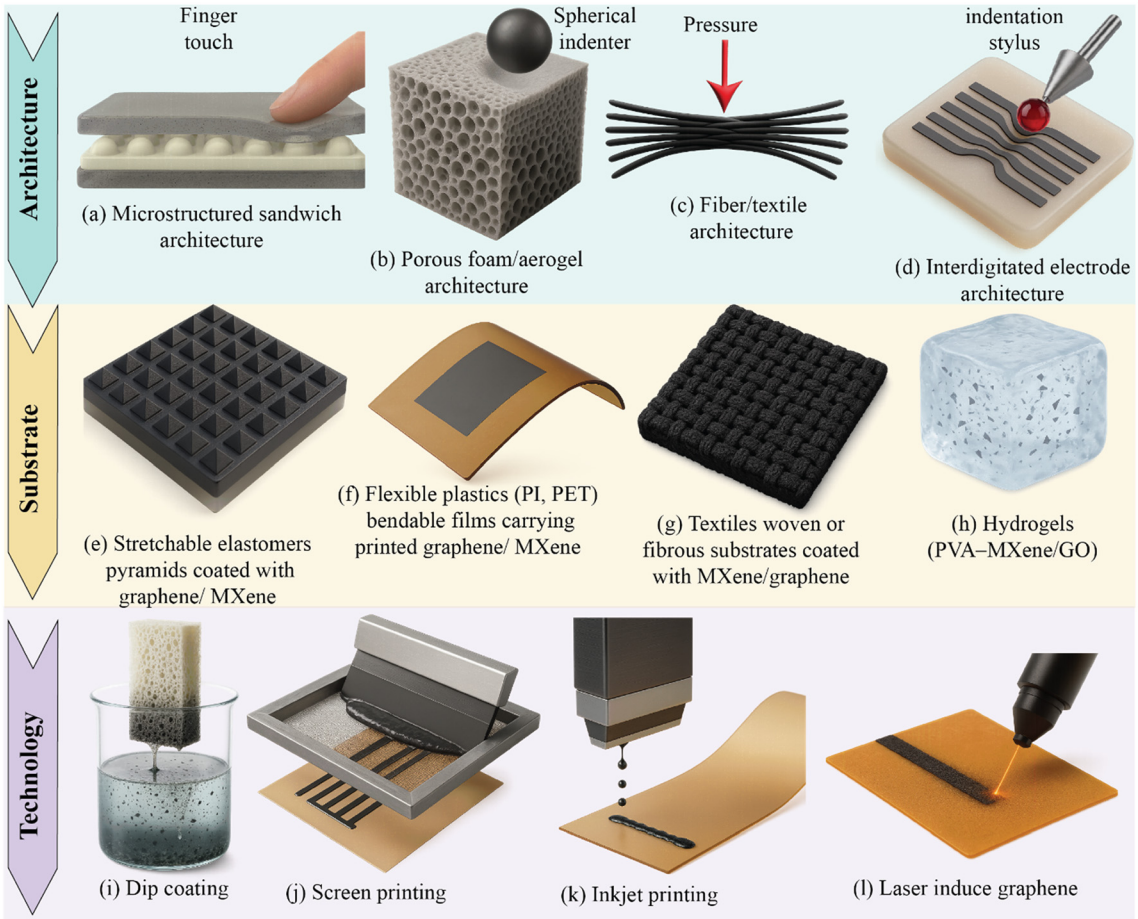

Fig. 4 Summary of the key MXene/graphene pressure-sensor design pathways. (a) In microstructured sandwich architectures, applied pressure flattens microdomes, rapidly increasing real contact area and producing strong resistance or capacitance changes. (b) In porous foams/aerogels, compression shrinks pore volume and shortens conductive percolation paths, increasing contact density and lowering resistance. (c) In fiber/textile systems, pressure tightens contact at yarn cross-points, enhancing inter-fiber coupling and creating local piezoresistive drops. (d) In interdigitated electrodes on soft substrates, vertical loading thins the elastomer and reduces finger spacing, strengthening tunneling and fringe-field effects. (e) Stretchable elastomers (PDMS, Ecoflex, and PU) coated with MXene/graphene. (f) Flexible plastics (PI and PET) printed or coated conductive layers. (g) Textiles and paper coated with MXenes/graphene. (h) Hydrogels (PVA–MXene/GO). (i–l) Fabrication routes—including dip-coating, screen printing, inkjet printing, and laser-induced graphene—enable scalable deposition and patterning for flexible pressure-sensor manufacturing.

sponges maintain their ability to compress deeply while withstanding high pressure forces and display linear deformation patterns before they return to their initial state after pressure release. MXene is commonly introduced by dip-coating or infiltration so that conductive flakes coat the internal skeleton of the foam, while graphene-based foams can be grown by CVD on a sacrificial template or formed by coating/reducing GO.[49,88,89] Moreover, the combination of MXene aerogels with other films in layered porous variants enables the control of linearity while their lightweight structure and permeability make them suitable for wearable applications. As a result, the 3D percolating structure of these materials allows them to function under various pressure conditions and maintain their performance through multiple operational cycles.

- Fiber/textile architectures: MXene or graphene is coated onto, printed onto, or embedded within fibers (cotton, elastic yarns, and PU), turning them into pressure/strain-sensing yarns that can be knitted or woven into pressure-sensitive fabrics (Fig. 4c).[90,91] The yarn crosspoints experience elevated local pressure that enhances contact surface area while reducing electrical resistance to form a piezoresistive "pixel". In addition, the direct printing of graphene inks onto fabrics results in e-textiles while MXene forms strong bonds with textiles through hydrogen bonding to create long-lasting sensing fabrics. Additional composite or spacer layers can be added around the yarns to amplify the local deformation and improve signal strength, while still keeping the whole structure wearable and washable. Consequently, the wide distribution of textiles across large areas allows this architecture to achieve body-conformal pressure mapping and support extended mechanical cycling.
- Interdigitated electrodes on soft substrates: interlocking conductive fingers (graphene screen-printed on PDMS, or patterned MXene *via* inkjet/screen printing) are laid on an elastomeric substrate (Fig. 4d).[73,92] Under applied pressure,

the application of pressure reduces the substrate thickness while moving the fingers closer together which enhances tunneling/fringe conduction and decreases resistance or changes fringe capacitance. The strain sensing geometry can be adapted to develop 2D tactile arrays for spatial pressure mapping through the placement of multiple interdigitated cells in a side-by-side configuration. MXene and graphene patterning and printing capabilities with high lateral resolution enable this design to be manufactured at a scale and used for flexible electronic circuit development.

- Multilayer/hybrid stacks: multiple functional layers are laminated so that different transduction modes coexist in one device. For instance, the literature has proven the feasibility of dual-mode stacks which use triboelectric materials on top of piezoresistive materials for detecting both dynamic contact–separation events and quasi-static loads.[93] Likewise, a PVDF piezoelectric film with MXene electrodes can be placed above a MXene/foam resistive layer, so one channel captures fast, transient events and the other captures quasi-static pressure, without adding large thickness or rigid backing.[94] MXenes and graphene need thin TPU or polyimide encapsulation layers to protect them against environmental factors and achieve uniform stress distribution in the stack.

Overall, the five recurring architectures (microstructured film/sandwich, porous foam/aerogel, fiber/textile, interdigitated planar, and multilayer hybrid) correspond to the fundamental sensing methods. These include sandwich cells for capacitive or controlled piezoresistive measurements and foams/aerogels for piezoresistive measurements across broad compression ranges, as well as, textiles/yarn networks for piezoresistive or triboelectric sensing in wearable applications and interdigitated layouts for resistive or capacitive operation with precise spatial control and hybrid stacks that unite static and dynamic channels within a single laminate.[34,95] The selection between MXenes and graphene depends on these form factors because these materials share solution-processability and printability and flexibility but respond differently to architectural designs. MXenes bond well with porous materials and textiles through dispersion and coating methods but graphene's thin atomic structure and printable patterns make it suitable for creating thin microstructured layers and detailed interdigitated electrodes. The system operates effectively only when it receives particular application guidance for its operation (skin-level micro-pressure sensing, wide-range load mapping, soft robotic grip, *etc.*). This issue is therefore addressed in the following section rather than here.

4.2 Substrates and matrices

The substrate or matrix provides mechanical support and flexibility and stretchability through four main categories. (i) In particular, the skin-like stretchable rubber materials PDMS Ecoflex and polyurethane serve as popular choices because they can be patterned into domes or pyramids for high sensitivity and they conform to surfaces while supporting conductive layers (Fig. 4e).[72,82,96] For example, graphene is commonly transferred onto PDMS to create crack-based ultrahigh-sensitivity films or used as a wrinkled/stretchable electrode after pre-strain release.[96,97] Similarly, MXenes can also be dispersed in PDMS, though their hydrophilicity *vs.* PDMS hydrophobicity means that surfactants or polymer binders (*e.g.* PVA and PU) are often added to stabilize the network.[98] PU foams are essentially porous elastomers and act as compressible piezoresistive sponges for MXenes or graphene; Ecoflex, an ultra-soft silicone, allows intimate skin contact for wearable patches.[82,99] In contrast, (ii) plastics (PI and PET): these films are bendable but not stretchable, and useful when only flexing is needed. Polyimide (PI) supports printed graphene patterns or spin-coated MXene films (Fig. 4f). PET commonly receives transferred CVD graphene as a transparent, flexible electrode, or drop-cast MXenes (with adhesion treatment).[100–102] Accordingly, such substrates suit bendable pressure sensors embedded in flexible circuits. Moreover, (iii) textiles and paper: MXene coatings on fabrics (cotton and polyester) create pressure-sensitive smart fabrics that are breathable because MXenes bond to cellulose through hydrogen bonds and similar applications use graphene inks printed on fabric materials (Fig. 4g).[95] The paper-based capacitive sensors consist of paper as the compressible dielectric/substrate material which is combined with printed or coated conductive electrodes (*e.g.*, AgNWs and carbon/graphene) to create ultralow-cost devices. Furthermore, all-paper stacks can also be realized by pairing conductive paper electrodes (*e.g.*, polypyrrole-printed paper or MXene-coated tissue) with blank tissue paper as the dielectric.[103–105] Finally, (iv) hydrogels: PVA hydrogels loaded with MXene sheets create conductive pressure sensors that are soft and water-rich and suitable for skin contact because their resistance changes when compressed and they can detect both pressure and temperature variations (thermo-piezoresistive) (Fig. 4h).[106] In addition, hydrogels function as ionic electrodes in capacitive sensors while MXenes and graphene oxide show good dispersion properties in these materials although MXenes tend to oxidize more quickly when exposed to water.[107] Overall, across all classes, substrate mechanics directly tune responses: a very soft, low-modulus matrix (porous silicone and foam) gives large deformation and high low-pressure sensitivity, while stiffer or multilayer stacks extend the usable range by preventing full collapse at higher loads. MXenes' surface chemistry affects their behavior because the –O/–OH terminations create hydrogen bonds that enhance adhesion to fibrous or polar or hydrogel matrices, which leads to better cycling stability. By comparison, the physical encapsulation or *in situ* reduction of GO within a polymer serves as the main method to stabilize graphene because it lacks active surface groups.[95]

4.3 Processing and integration methods

The method of MXene or graphene integration into pressure sensors determines how well the materials distribute evenly and

how consistently they perform and how easily they can be mass-produced. In this context, the integration methods for pressure sensors include coating, printing, microfabrication and roll-to-roll manufacturing.[108] The dip-coating method of PU foams and textiles into MXene ink solution produces a uniform coating that covers the entire porous structure (Fig. 4i),[95] whereas, spray-coating or airbrushing MXenes/graphene onto PDMS microdomes produces targeted coverage.[109] The vacuum-assisted filtration method enables the creation of dense uniform films from MXenes or graphene oxide which can be transferred to flexible substrates.[110] Similarly, drop-casting and spin-coating methods allow MXene or graphene inks to be deposited onto flexible substrates, enabling the formation of uniform conductive layers for pressure sensing applications.[111] The printing techniques enable large-scale pattern creation because MXene and graphene nanoplatelet inks can be used to create interdigitated or textile-integrated electrodes (Fig. 4j).[112,113] The screen-printing process allows users to create features with dimensions between 30 and 50 μm when using MXene inks that contain binders. By comparison, the precision of inkjet printing depends on MXene ink formulations which need to prevent both restacking and graphene nozzle blockage (Fig. 4k).[114] Microfabrication techniques allow scientists to build exact functional microstructures through photolithography which creates patterned graphene electrodes.[115] The method of laser induced graphene structuring enables researchers to create precise patterns on polymer materials, while direct high-precision printing and post-patterning techniques exist for flexible systems (Fig. 4l).[112] The production of flexible sensors using roll-to-roll (R2R) printing of graphene inks on PET substrates has been achieved at industrial scales,[116] and researchers propose similar continuous coating and infiltration methods for MXenes when ink stability and drying control and MXene oxidation management are achieved.[117] The application of thin PU or PVA encapsulation protects MXenes from oxidation and graphene from abrasion while maintaining flexibility.[118] The sensor requires printed conductive traces or low-temperature silver paste for lead attachment to establish electrical connection and, multilayer stacks need correct alignment during lamination procedures. The different fabrication methods range from laboratory spin-coating to industrial R2R printing, yet researchers face difficulties in creating uniform microstructures and protecting MXenes from degradation throughout processing.

4.4 Environmental and biocompatibility considerations

The development of MXene and graphene pressure sensors for wearable applications requires equal attention to electrical performance, environmental tolerance, safety regulations and user comfort standards.[119] Moreover, the combination of water and sweat exposure creates significant stress on these materials because MXenes ($Ti_3C_2T_x$) experience rapid oxidation when exposed to oxygen and water, which accelerates performance degradation and induces sensing signal drift, thus requiring protective coatings to prevent skin contact failure within short periods.[16] In addition, the addition of thin waterproof flexible encapsulation materials (parylene, PU and PDMS) helps protect MXene-based fibers from degradation while artificial sweat exposure does not affect their stability.[120] Conversely, the resistance of graphene remains stable in moisture but water accumulation in microcracks and interfaces causes temporary resistance changes and capacitive sensors experience dielectric constant shifts which affect pressure measurement accuracy, thus requiring breathable platforms with porous structures (foams and textiles) for sweat drainage.[121] Furthermore, the primary factor that causes long-term reliability problems for MXene materials is oxidation which leads to drift in their performance. The influence of oxidation in MXenes and moisture accumulation in cracked graphene on signal stability, together with the mitigation provided by encapsulation of MXenes and by maintaining dry interfaces in graphene, is schematically illustrated in Fig. 5a and b. The PVA polymer–MXene combination establishes an oxygen-free space which makes the material more stable for longer periods (the PVA/MXene film showed improved conductivity retention compared to water-based MXene films which lost their conductivity after one to two weeks).[121] Additionally, the resistance of polymer materials changes with temperature while their thermal expansion properties affect sensor readings. MXene films show metallic properties which enable transport measurements but graphene-based elements need temperature sensors or protective packaging to operate at stable temperatures because of their high temperature coefficient of resistance (TCR) values.[16] Therefore, the development of safe wearable devices needs appropriate management of these factors to achieve biocompatibility. The encapsulation process enables graphene films to become safe for skin contact but high exposure to loose graphene flakes through inhalation becomes dangerous. Notably, the 24 hour cytocompatibility test of skin fibroblasts (L929) with MXene hydrogel composites showed positive results in laboratory tests, and standard encapsulation methods protect these materials for skin contact application.[122] Consequently, all wearable sensor implementations require protective packaging which serves dual purposes to maintain electrical stability and ensure user safety. The protective layers of PDMS, Ecoflex, TPU and parylene serve two purposes by protecting MXenes from oxidation and graphene from damage, while making textile sensors washable and securing electrical connections with conductive epoxy and silicone strain relief. However, the sensitivity of capacitive devices decreases when they use stiff encapsulation materials, which also reduces their ability to detect pressure changes.[120] Finally, the last requirement for wearable technology needs to ensure that users can operate it comfortably. Thin graphene-on-polymer films with 2 μm thickness create an electronic tattoo experience while MXene-coated fabrics maintain regular fabric texture but MXene powder becomes irritating when it separates from the fabric unless proper sealing occurs.[123] Thus, the design of wearable technology needs to be both lightweight and breathable because these characteristics enable users to stay safe while feeling comfortable.[124] Overall, the chemical stability of graphene

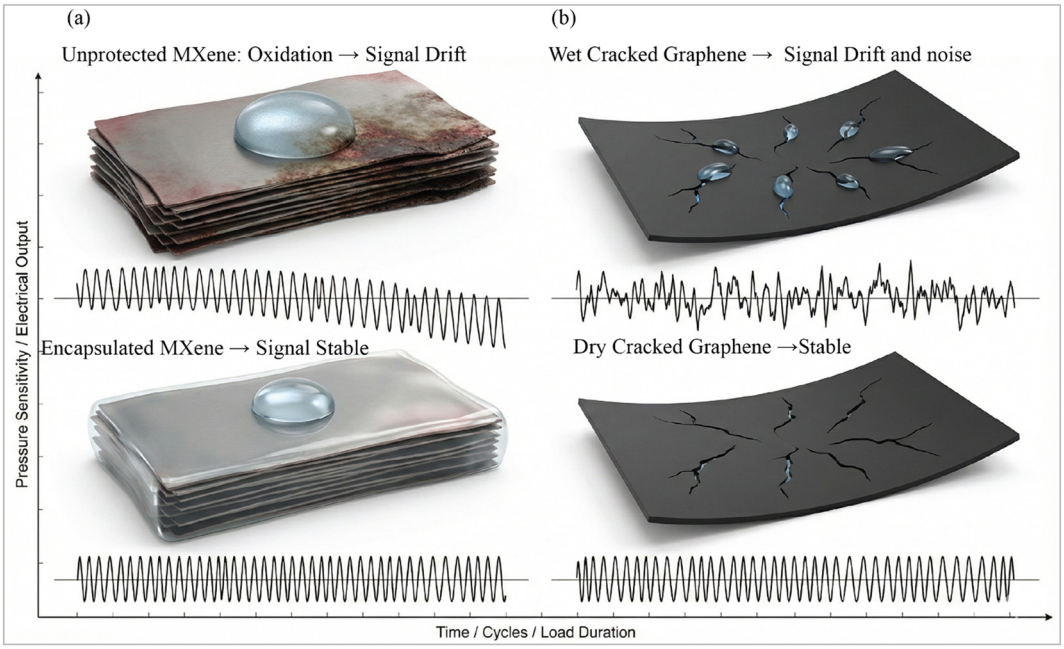

Fig. 5 Schematic illustration of humidity-induced signal instability in MXene- and graphene-based pressure sensors. (a) Unprotected MXene exposed to water/oxygen undergoes surface oxidation, leading to pronounced signal drift, whereas an encapsulated MXene stack shows a stable electrical response. (b) Wet cracked graphene with moisture trapped in interfacial cracks exhibits signal drift and noise, while the same cracked graphene film in a dry state provides a stable output.

makes it suitable for extended on-skin applications, yet MXenes require protective encapsulation to stop their oxidation-based performance degradation, and cracked graphene structures demand careful control of moisture so that interfacial regions remain dry and signal drift is avoided. The combination of suitable encapsulation methods with breathable designs enables both materials to achieve safe, biocompatible and comfortable wearable prototypes for real-world applications.

5. Data extraction table (literature landscape)

Table 1 presents recent flexible pressure-sensor examples which use piezoresistive, capacitive, piezoelectric and triboelectric sensing mechanisms with graphene and MXenes and their hybrid materials. Additionally, the table presents device architecture types (flat films, porous foams/aerogels, micro-textured dielectrics, and textiles) with their respective performance metrics which include kPa^{-1} sensitivity, V kPa^{-1} sensitivity, Pa detection limits, Pa to MPa linear/usable range, hysteresis, response time in ms and cycling endurance. Together, the design map provides a step-by-step process to pick mechanisms based on DC or AC signal types and material families for ultra-low pressure or tens–hundreds of kPa operation followed by selecting an architecture and packaging to achieve the best possible design under budget constraints. Accordingly, the design trade-offs between mechanisms show direct relationships with specific use-cases according to the table. The piezoresistive graphene micro-architectures with vertical micro-pyramids, LIG on micro-textured PDMS and LM-tuned sponges achieve high per-pascal sensitivity in the sub-kPa range (10^2–10^3 kPa^{-1} with Pa-level LOD), which enables them to detect pulse and throat micro-motion and soft touch events. However, the main drawback of these sensors is their restricted linear operation range (less than 1–5 kPa) and increasing hysteresis because of crack propagation and interface slipping. The piezoresistive MXene composites operate with average sensitivity but they provide extensive linear operation from Pa to hundreds of kPa while maintaining excellent cycling stability (10^3–10^4+). Thus, the sensors operate best for posture, plantar, grip and seat applications because they provide excellent repeatability even though their sensitivity is not the highest.

The capacitive stacks consisting of MXene–polyvinylpyrrolidone (PVP) membranes, MXene (PVDF-TrFE) scaffolds and graphene-coated porous PDMS operate with minimal hysteresis and drift while requiring no power consumption for detecting forces from Pa to 10^2–10^3 kPa. Meanwhile, the piezoelectric PVDF-TrFE devices with MXene or rGO/multi-walled carbon nanotube (MWCNT)/poly(3,4-ethylenedioxythiophene) (PEDOT) electrodes function as self-powered AC sensors which detect rhythmic biosignals including pulse wave velocity and respiration. The devices detect AC signals but fail to detect DC forces while showing linear voltage–pressure relationships and delivering high signal-to-noise ratios.

The triboelectric devices (TPU/$BaTiO_3$/MXene, 3D graphene foams and graphene-based triboelectric nanogenerator (GT-TENG)) function as event sensors and micro-energy harvesters which use open-circuit voltage (VOC)/short-circuit current (ISC) signals to detect taps and steps but they do not produce DC power. In all cases, the two main factors which affect all sensor

Table 1 Comparative performance of MXene- and graphene-based flexible/stretchable pressure sensors (2021–2025)

Material system	Sensing mechanism	Device architecture	Usable pressure range/regime	Limit of 2detection	Peak sensitivity	Hysteresis/stability	Cycling durability	Primary application fit (static/dynamic)
MXene/polypyrrole (PPy)@PDMS sponge[49]	Piezoresistive	MXene/PPy-coated porous PDMS foam	0.43 Pa–275 kPa (touch → high load)	0.43 Pa	6.89 kPa^{-1} (<15 kPa)	~10% hysteresis at max load; negligible drift across test	5000+ cycles stable	Posture & motion (static + dyn)
Vertical graphene micro-pyramids[125]	Piezoresistive	Vertically grown graphene on a micro-pyramid array	0.1–100 kPa (wide, near-linear)	100 Pa	131.36 kPa^{-1} (<0.1 kPa)	Low hysteresis; stable wearable signals	>10 000 cycles	Wearable touch/robotic tactile (static + dyn)
Cross-linked rGO aerogel[126]	Piezoresistive	Hyperelastic rGO aerogel (buckling/honeycomb microstructure)	Up to ~250 kPa (≤70% compression)	≈500 Pa	121.45 kPa^{-1} (<2.5 kPa)	No obvious hysteresis or drift, even under high compression cycling	20 000 + cycles	HMI/motion control (dyn)
MXene–PVP nanofiber mat[127]	Capacitive	Electrospun MXene–PVP membrane as a compressible dielectric	~9 Pa–200 kPa (to 0.2 MPa)	~9 Pa	0.5 kPa^{-1} ($\Delta C/C_0$ kPa^{-1}, 0–1.5 kPa)	No significant hysteresis; stable signal after thousands of cycles	8000 cycles (<5% drift)	Pulse/joint/map (static + dyn)
TPU/$BaTiO_3$/MXene[128]	Triboelectric	TPU/BTO/MXene composite + PDMS + AgNW electrodes separation	0.04–113 kPa (two regimes: 0.04–10 kPa and 10–113 kPa)	40 Pa	4.6 V kPa^{-1} 2(0.04–10 kPa) 2.5 mA kPa^{-1} (0.04–10 kPa)	Stable, low hysteresis ($\tan\delta \approx 0.24$); retains output under ≈60% strain; >100 cycles without degradation	>100 cycles with stable charge (≈2.17 mC m^{-2}) under 60% strain and 113 kPa	Heartbeat, respiration, voice, gestures, robotics (dyn contact)
PVDF-TrFE/MXene ($Ti_3C_2T_x$)[129]	Piezoelectric	Electrospun aligned nanofibrous film sandwiched between Al electrodes, encapsulated with polyimide tape	Linear regime up to 20 N@1 Hz (~0–50 kPa equivalent)	≈50 000 Pa	VOC ≈ 1.58 V@20 N, ≈3× higher than pure PVDF-TrFE; power density ≈3.64 mW m^{-2}	Linear voltage–pressure response; negligible triboelectric interference; stable under sinusoidal loading	>1000 cycles	Self-powered e-skin and wearable sensing – (dyn)
PVDF-TrFE/rGO–MWCNTs/PEDOT[130]	Piezoelectric	rGO–MWCNT-doped PVDF-TrFE nanofibers coated with PEDOT	1 Pa–25 kPa (two regimes: <1 kPa high-sensitivity, 1–25 kPa moderate)	1 Pa	19.09 kPa^{-1} (<1 kPa), 0.429 kPa^{-1} (1–25 kPa)	Stable I–V behavior; linear output; repeatable under dynamic/static loading	>10 000 cycles	Heartbeat, pulse, voice, chewing, eye blink (self-powered e-skin) (dyn)
Graphene-coated PDMS porous foam[131]	Capacitive	Sugar-templated PDMS foam coated with graphene flakes on pore walls between carbon electrodes	0–12 kPa (high sensitivity below 6 kPa)	≈50 Pa	0.137 kPa^{-1}, detection limit ≈50 Pa	Low hysteresis, stable output after repeated loading	Stable for >100 cycles at 4 kPa without degradation	Dynamic biomedical sensing – respiration, finger taps, swallowing
3D graphene foam[132]	Triboelectric	3D porous graphene foam/PET	Not specified (mechanical contact, 3 Hz operation)	—	V_{oc} ≈ 400 V, I_{sc} ≈105.7 μA, power density ≈10.37 W m^{-2}@40 MΩ	Stable under repeated compression	>15 000 cycles, retained >95% output	Dynamic energy harvesting & self-powered sensing (mechanical motion, autonomous systems)
MXene ($Ti_3C_2T_x$)/PVDF-TrFE composite nanofibrous	Capacitive	Electrospun MXene/ PVDF-TrFE nanofiber	0–400 kPa (linear region up to	1.5 Pa	0.51 kPa^{-1} (0–1 kPa),	Negligible hysteresis; stable low-pressure	>10 000 cycles at 167 kPa, >95%	Dynamic physiological

Table 1 (continued)

Material system	Sensing mechanism	Device architecture	Usable pressure range/regime	Limit of 2detection	Peak sensitivity	Hysteresis/stability	Cycling durability	Primary application fit (static/dynamic)
scaffold[133]		dielectric layer sandwiched between poly(3,4-ethylenedioxythiophene: poly(styrene sulfonate (PEDOT:PSS)/PDMS electrodes	~150 kPa)		detection limit 1.5 Pa	response; minimal drift under 167 kPa load	signal retention	monitoring – pulse, respiration, muscle/eye motion, phonation sensing
PVA/SWCNT/MXene composite film[134]	Piezoresistive	Wrinkled double-layer film of PVA/SWCNT/MXene	0–130 kPa (high sensitivity <1 kPa)	<1 Pa	1131.87 kPa^{-1} (<1 kPa); 54.71 kPa^{-1} (1–10 kPa); 7.28 kPa^{-1} (10–40 kPa); 2.1 kPa^{-1} (40–130 kPa)	Highly stable; <3% variation after 7000 cycles; fast response/recovery ≈12.5/12.8 ms	>7000 cycles, stable $\Delta I/I_0$ response	Dynamic wearable sensing – pulse, speech, and finger/robotic joint motion monitoring
MXene/PDMS @PTFE/PVA[135]	Triboelectric	Alk-MXene/PDMS composite friction layer with a single-electrode TENG architecture	0.94 Pa–159 kPa	0.94 Pa	1.48 V kPa^{-1}	Negligible drift	>10 000 cycles	Dynamic wearable sensing, motion & object recognition

designs include structural design (foams/aerogels for wide span and durability and films for low-pressure sensitivity) and packaging materials (thin PDMS/Ecoflex/TPU or parylene for contact stabilization and MXene oxidation protection).

The selection of sensors depends on specific requirements because graphene microstructures work best for lightweight signals, MXene composites and capacitive stacks excel in wide-range applications, and piezo and tribo devices suit AC and self-powered and "sense-and-harvest" applications. Moreover, the 1–5 scores in the radar plots represent ordinal ratings which translate the qualitative–quantitative trends into numerical values, where 1 indicates weak performance and 5 indicates excellent performance (Fig. 6). The sensitivity and LOD of graphene micro-architectures received the highest ratings but their pressure range, linearity, hysteresis and endurance received lower ratings. The MXene composites and capacitive stacks received better ratings for their wide operational range and stable performance, and piezoelectric and triboelectric mechanisms achieved top marks for their fast response times. Finally, the unitless comparison table shows the essential trade-offs between different materials and sensing methods.

6. Performance comparison between graphene and MXene pressure sensors

The study describes performance evaluation through Fig. 7a–f which we review before comparing MXene and graphene flexible pressure sensors. In this context, the rate of electrical signal change per pressure unit appears as $(\Delta R/R_0)/\Delta P$ or $(\Delta C/C_0)/\Delta P$ in kPa^{-1} for resistive/capacitive devices to measure sensitivity. Meanwhile, piezoelectric and triboelectric sensors achieve their output performance by detecting touch and vibration dynamics through voltage and current measurements. In all cases, the sensor operates within a specific pressure range, which enables stable and non-saturated responses to changes in pressure. Specifically, the sensitivity of graphene crack-network films reaches its highest point when operating under low pressure conditions but their performance deteriorates when they experience increased loads. By comparison, the mid to high pressure range of MXene-based porous and foam structures shows quasi-linear behavior while surviving multiple loading cycles, which makes them suitable for grip force and plantar/weight mapping applications. Additionally, the encapsulation process protects MXenes from oxidation when they operate under humid or sweat-exposed conditions.

6.1 Sensitivity comparison (low *vs.* mid *vs.* high pressure)

The sensitivity divides values into three pressure ranges which included low (<10 kPa), mid (10–100 kPa) and high (>100 kPa) pressure zones.[64] Specifically, the MXene-based devices against graphene-based devices through three pressure zones matched the sensitivity curves shown in Fig. 7a and b. Structurally, the

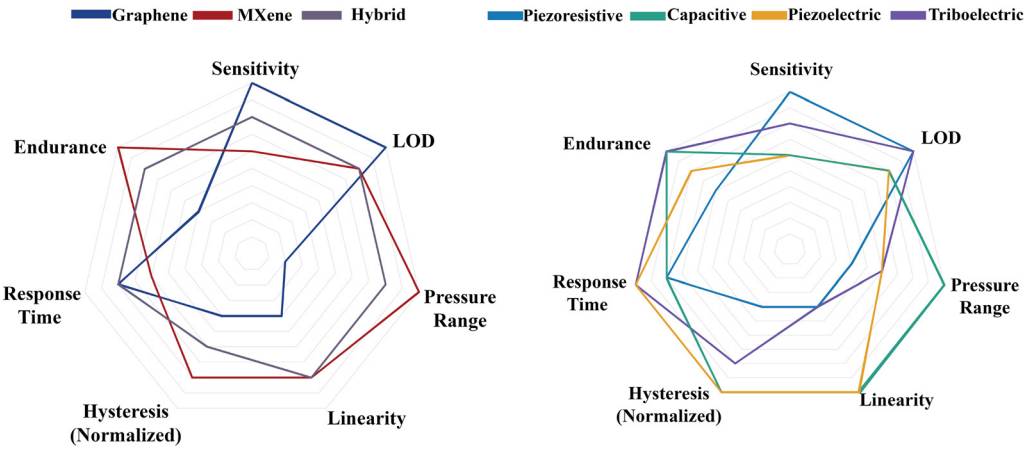

Type	Name	Sensitivity	LOD	Pressure Range	Linearity	Hysteresis (Normalized	Response Time	Endurance
Material	Graphene	5	5	2	2	2	5	3
Material	MXene	3	4	5	4	3	4	4
Material	Hybrid	4	4	4	3	3	4	4
Mechanism	Piezoresistive	5	5	3	3	2	5	3
Mechanism	Capacitive	3	4	4	4	4	3	4
Mechanism	Piezoelectric	4	4	3	4	5	5	5
Mechanism	Triboelectric	4	3	4	2	2	5	4

Fig. 6 Normalized performance comparison of material families (graphene, MXenes, hybrids) and sensing mechanisms (piezoresistive, capacitive, piezoelectric, and triboelectric) across seven key metrics—sensitivity, LOD, pressure range, linearity, hysteresis, response time, and endurance using a 1–5 ordinal scale derived from consolidated literature trends.

hierarchical structure of $Ti_3C_2T_x$ MXene assemblies forms conductive paths through line and point contacts which improve their sensitivity when measuring mid to high pressure applications. For example, the MXene textile structure showed 1.16 kPa^{-1} sensitivity across the 1.5 MPa pressure range because the MXene strongly bonded to chitosan fibers while showing no significant decrease in performance during multiple testing cycles. Furthermore, the MXene composite materials demonstrate high sensitivity across various low-pressure ranges because the study achieved optimal junction density and controlled porosity levels (1.13×10^3 kPa^{-1} at <1 kPa, 54.7 kPa^{-1} at 1–10 kPa, 7.28 kPa^{-1} at 10–40 kPa and 2.1 kPa^{-1} at 40–130 kPa).[136] In contrast, the graphene-based sensor with microcrack and porous structures achieves its peak sensitivity at low pressures because its contact area expands quickly when it first experiences compression. The seven-layer rGO-coated silk textile demonstrates 2.58×10^3 kPa^{-1} sensitivity between 0.2 kPa and 72.3 kPa. However, the laser-scribed graphene foam sensor shows 0.96 kPa^{-1} sensitivity at 50 kPa but its sensitivity drops to 0.005 kPa^{-1} when the contact reaches its highest point above 50 kPa. The sensitivity of these materials shows high initial gain because of crack closure but their sensitivity decreases when pressure increases.[64,137] The rGO fabric shows high sensitivity at low pressure measurements but its sensitivity drops to 3.82 kPa^{-1} when testing pressures between 10.9 and 91.3 kPa and further decreases to 1.84 kPa^{-1} when testing pressures between 72 and 421 kPa. Consequently, the linear sensitivity range of these materials decreases when they experience increasing pressure loads. By comparison, the MXene textiles and aerogels show unaltered high sensitivity throughout all pressure tests, yet graphene foams with porous or laser-scribed structures demonstrate reduced sensitivity when exposed to high pressure.[64,137]

In summary, the sensitivity of graphene materials reaches its peak at low pressures below 10 kPa but their performance decreases when pressure increases. In contrast, the MXene aerogels and textiles show sensitivity responses between 10 and 100 kPa and reach above 100 kPa while maintaining sensitivity values of 1.16 kPa^{-1} from 1.5 MPa. Moreover, MXene materials show high sensitivity at low pressures, yet their performance remains excellent at intermediate pressures through modifications of their porosity and junction density. Therefore, the sensitivity of graphene materials excels at detecting light touch and biophysical signals but MXene materials perform better for robotic applications that need wide operating ranges and long-lasting durability.

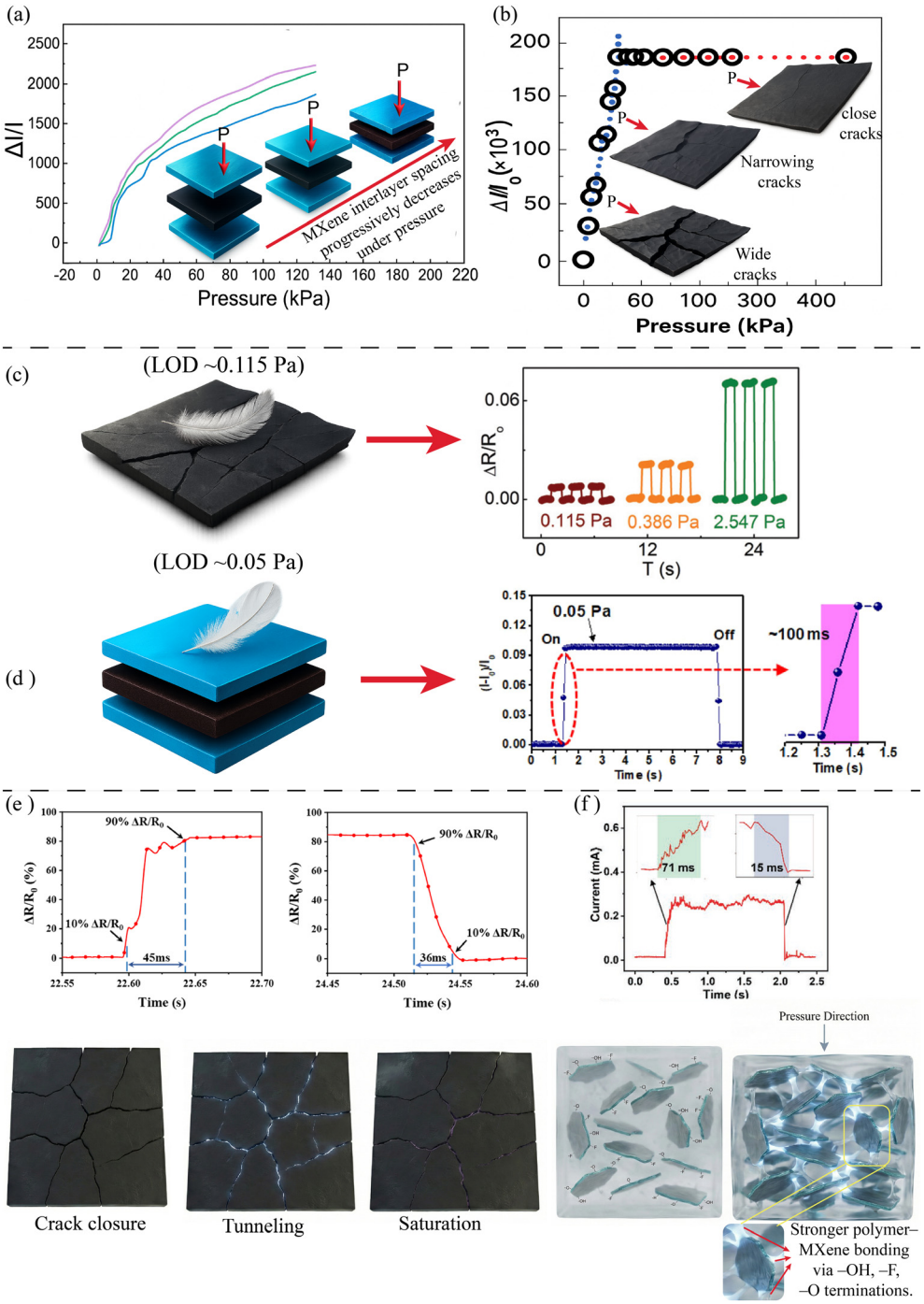

Fig. 7 Performance comparison of graphene- and MXene-based pressure sensors. (a and b) Sensitivity behavior of crack-engineered graphene films and MXene porous/textile architectures across low-, mid-, and high-pressure regimes. (c and d) Sub-pascal limit of detection and small-load sensing demonstrated by representative graphene- and MXene-based devices. (e) Graphene crack-network response under lateral compression, where crack closure and formation of tunnelling paths produce a rapid (~45 ms) change in resistance and hysteretic recovery. (f) MXene aerogel/foam response under compression, where viscoelastic relaxation of the soft matrix and evolution of a resilient percolation network—stabilised by MXene surface terminations (–O, –OH, and –F)—delay saturation and sustain sensitivity under large compression.

6.2 Limit of detection

For clarity, detection limits are discussed in pascal (Pa), while operational pressure ranges are reported in kilopascal (kPa) or megapascal (MPa) depending on the application regime. The LOD is the smallest pressure variation which produces detectable output changes in flexible pressure sensors as shown in Fig. 7c and d, which shows typical LOD behavior for graphene and MXene devices. In particular, state-of-the-art devices achieve single-pascal or sub-pascal detection capabilities which allow

them to detect small objects and physiological pulses.[138] More specifically, the detection limits of graphene-based pressure sensors extend from 0.1 Pa to 5 Pa because previous studies have developed two different sensor types, including micro-patterned graphene/PDMS capacitive sensors and reduced-graphene-oxide foam sensors.[138] The detection range of graphene sensors extends from 0.1 Pa to 5 Pa but most devices operate between sub-pascal and a few-pascal levels; the measurement results depend on the sensor design and testing environment.[138] Similarly, the detection limits of MXene sensors reach extremely low values because thermopiezoresistive MXene/polyethylene oxide (PEO) aerogels detect 0.05 Pa pressures and MXene/cetyltrimethylammonium bromide (CTAB)/cellulose microfiber (CMF) composites detect 0.1 Pa pressures while MXene foams detect pressures at 4.6 Pa.[65] The detection range of MXene sensors extends from 0.05 Pa to multiple pascals but specialized MXene aerogels achieve sub-pascal detection.[65] Overall, the detection limits of both materials reach below 1 pascal while they can detect biological signals.[65,138] The detection system reaches sub-pascal sensitivity through its combination of graphene structures with cracks and MXene aerogels which show excellent compressibility properties. For example, the reduced-graphene-oxide foam sensor detects 0.2 Pa changes while the thermopiezoresistive MXene/PEO aerogel sensor detects 0.05 Pa pressures.[65,138] Ultimately, the detection threshold of practical sensors depends on material properties and external interference from mechanical noise and electronic interference which reduces the detectability of small pressure changes.

6.3 Response and recovery time

The mechanical relaxation properties of soft materials control sensor response speed instead of MXene or graphene conductivity according to Fig. 7e and f. Specifically, the nanofiber-reinforced MXene–graphene aerogel sensor showed 71 ms response time and 15 ms recovery time with 17 000 cycle stability but the wearable graphene piezoresistive sensor required 45 ms to respond and 36 ms to recover.[69,139] Overall, the response and recovery times of graphene piezoresistive and capacitive pressure sensors range from tens to hundreds of milliseconds. The wearable graphene sensor achieved 45 ms response time and 36 ms recovery time while other devices operated between 18 and 80 ms based on their microstructure design. In contrast, the graphene electrodes in triboelectric e-skins achieve sub-10 ms response times because the smart e-skin responds in 1.4 ms.[69,139] Similarly, MXene piezoresistive sensors achieve their response time based on their structural design because nanofiber-reinforced aerogels detect changes in 71 ms while showing a 15 ms recovery period,[139] and AgNW/MXene aerogels detect changes in 60 ms,[140] gas-foamed MXene aerogels detect changes in ~11 ms,[58] and dual-modal MXene/cellulose nanofiber (CNF) aerogel sensors detect changes in 4.71 ms while recovering in 2.99 ms.[141] For instance, the MXene/CNF aerogel sensor needs 4.71 ms to respond but the triboelectric graphene e-skin sensor reacts in 1.4 ms.[141]

Regarding durability, the material properties of sensors show a distinct pattern regarding their durability because MXene sensors prove highly resistant to wear. The nanofiber-reinforced MXene aerogels show enduring performance through 17 000 cycles,[139] gas-foamed MXene aerogels survive more than 25 000 cycles,[58] and AgNW/MXene aerogels maintain stability through 1000 cycles;[140] other MXene composites achieve multi-thousand stable operation cycles.[142] By comparison, the performance of graphene-based sensors remains stable through multi-thousand loading cycles but their exact number varies. A wearable graphene piezoresistive sensor operated for 2800 cycles before losing its stability,[69] while other devices operated between 500 and 10 000 cycles based on their design, and 3D graphene foam sensors maintained their performance through more than 10 000 cycles with minimal signal degradation.[143] Thus, the MXene and graphene sensors detect human touch at speeds below 100 ms but their piezoelectric/triboelectric electrode configuration allows them to respond in less than 10 ms. The combination of MXenes with other materials produces composites which maintain their performance through more than 10k cycles when subjected to wide-range loading but graphene crack-film sensors show exceptional sensitivity yet their performance degrades through time due to crack accumulation and hysteresis development.

The soft matrix determines response time through its viscoelastic relaxation and contact-network evolution instead of carrier mobility. Moreover, the surface terminations of MXenes (–O, –OH, and –F) create strong bonds with polymers, which produces durable percolation networks in aerogels and foams that extend their sensitivity under extensive compression. The stability of junctions determines durability but protective coatings must be applied to prevent oxidation. Conversely, the fast triboelectric sensing of graphene occurs because of its porous structure but its crack-network design makes it more susceptible to crack growth and signal drift during high-pressure operations. Therefore, the selection of MXene aerogels/textiles should occur for applications that need mid- to high-pressure operation with high cycle numbers, while graphene crack-films/foams should be used for ultra-low-pressure applications that require high sensitivity. Finally, the selection of readout mode between tribo/piezo and resistive/capacitive depends on the needed bandwidth range.

6.4 Limitations of pooling and comparison

Several caveats frame our comparisons. The papers lack standardization in their sensitivity measurements because resistive and capacitive sensors use $\Delta R/R_0$ and $\Delta C/C_0$ slope measurements for kPa pressure changes but piezoelectric and triboelectric sensors use different measurement units such as V N^{-1} and current-per-force (*e.g.* 0.0048 V N^{-1} (ref. 114)). Additionally, the authors used strain-type sensor gauge factor values only when they established direct connections between strain measurements and applied pressure. Second, different loading protocols exist between studies because authors employ

quasi-static compression ramps and rapid tapping methods which produce different results when testing viscoelastic materials at high speeds. We selected quasi-static data for analysis when they were available but we used the reported low-pressure window to estimate sensitivity for devices that did not show linear behavior and we indicated power-law behavior as strongly nonlinear. Third, many trends which seem to be between MXenes and graphene actually stem from design choices: MXenes find their way into thick 3D foam structures and aerogel and textile materials which naturally resist high loads and maintain their structure during extended cycling operations. Graphene serves as thin crack-network films to achieve maximum performance at low pressure levels. Thus, part of the contrast reflects design choices rather than intrinsic material limits; true head-to-head comparisons in identical geometries are rare. The fourth limitation stems from restricted statistical power because researchers have published only a few studies about graphene devices operating above 100 kPa, so we omitted statistical significance assessments. The research focused on detecting major scale differences across different measurement ranges while excluding specific performance bands that had matching values between 1 Pa and 10 Pa. Finally, the fifth factor demonstrates that scientists choose to publish only their most favorable results because they hide evidence of hysteresis, drift and durability problems; MXene oxidation becomes minimized through storage under inert conditions and short testing durations; researchers do not show how graphene films develop extended cracks during multiple cycling tests.

Overall, the two material platforms face multiple reporting and pooling problems which create challenges for translation. MXene sensors maintain their resistance to various mechanical stresses while providing stable measurement results under medium to high pressure conditions but $Ti_3C_2T_x$ MXene shows chemical instability because it oxidizes when exposed to humid or sweat-containing conditions and its conductivity changes with time, requiring protective coatings for skin contact which raises biocompatibility issues. Conversely, the graphene crack-network sensors maintain chemical stability when applied to skin while detecting minimal pressure changes below 10 kPa. The crack-based sensing mechanism of these sensors produces drift during multiple cycles while showing loading–unloading hysteresis, and it becomes saturated or non-linear when subjected to increased loads. Therefore, MXene devices need protection from moisture and oxidation to operate dependably in wearable applications, yet graphene devices need better mechanical strength and uniform operation under sustained pressure. Taken together, our research established design principles for these materials which include graphene performing best at ultralow-pressure detection while MXenes maintain useful responses and structural integrity at higher pressures and multiple cycles of operation. The detection limits of both materials reach the Pa range and their response times remain below 100 ms. The long-term operational stability of MXene composite materials exceeds that of other materials. Looking forward, future architectures (for example, oxidation-stable MXene skins or wide-range graphene foams) may blur or overturn these distinctions.

7. Material-selection framework (engineering decision map)

The research findings enable us to develop a system which helps engineers and researchers select suitable materials (MXenes *vs.* graphene) and detection methods for their specific application needs. In practice, the selection process requires engineers to consider both material properties and all application-specific requirements including the pressure range, signal type, durability needs and form factor constraints. Accordingly, the following section presents application domains with their corresponding sensor requirements followed by suggested material–mechanism pairs for each case. Ultimately, the selection process for a platform requires consideration of manufacturability and scalability factors, which leads to a four-panel material-selection decision map (Fig. 8a–d).

7.1 Mapping applications to sensing requirements

Let's consider a set of representative use-cases in wearable and robotic sensing, and outline their typical pressure profiles and key requirements:

- The wrist pulse patches for wearable blood pressure monitoring require sensors to detect low external pressures between 0.5 and 2 kPa on skin while handling dynamic pressure signals at 1 Hz frequency with static preload. Furthermore, the sensor needs to detect pressure changes of less than 1 kPa with high precision while maintaining thinness and breathability and using minimal power and enduring more than 1000 operational cycles.[144] The combination of PVDF piezoelectric strips with graphene electrodes enables pulse detection through voltage signals and shows natural aptness for dynamic pressure measurement.[145] Consequently, a solution for tracking both constant pressure values and additional pressure fluctuations requires a piezoresistive graphene sensor for static measurements and a PVDF piezoelectric sensor for detecting dynamic pressure spikes. The graphene element operates at a fixed baseline level while the piezoelectric element measures all pressure waves.[146] As a result, the dual-sensor configuration allows users to monitor cuff pressure and arterial pulse waveform data at the same time. The low-pressure detection capabilities of MXene aerogel sensors reach down to single-pascal and sub-pascal levels but their stability becomes a concern for extended wearable applications because they need protective encapsulation to prevent oxidation-related signal drift.[147,148] Moreover, the detection resolution of capacitive sensors reaches 1–2 Pa for pulse measurement but they experience problems with movement interference.[149] Therefore, the most dependable solution for detecting ultra-low-pressure dynamic signals involves using graphene-based piezoresistive skin because it provides stable baseline measurements and shows minimal drift during extended operation.

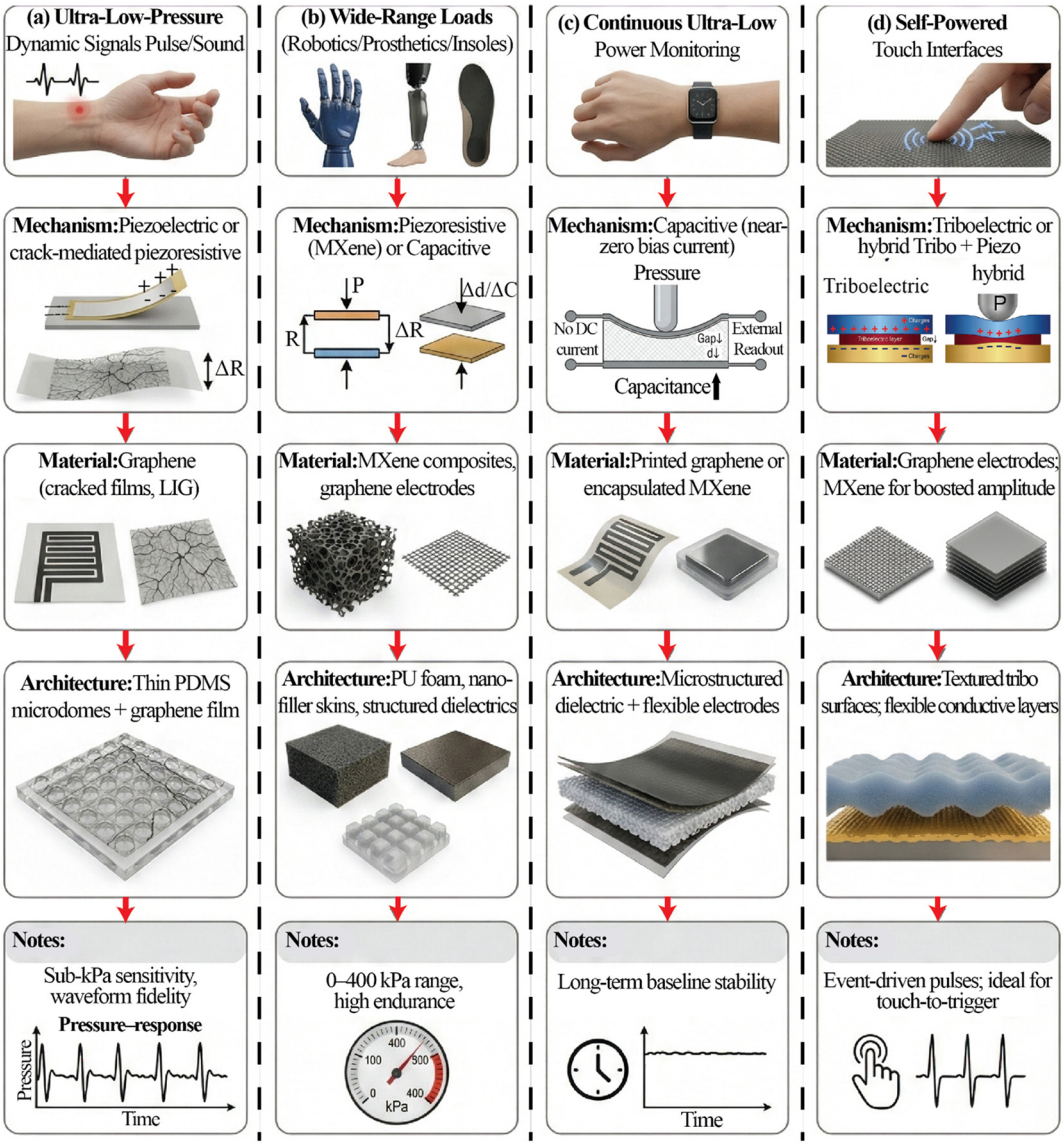

Fig. 8 Material-selection decision map for flexible pressure sensors (graphene *vs.* MXene architectures). (a) Ultra-low-pressure dynamic signals (pulse/sound) mapped to piezoelectric and crack-mediated graphene e-skins optimized for sub-kPa sensitivity and waveform fidelity. (b) Wide-range static and quasi-static loads in robotics, prosthetics and plantar/gait insoles, highlighting MXene-based foams/textiles and graphene electrodes for 0–400 kPa operation and high endurance. (c) Continuous ultra-low-power monitoring in moderate pressure regimes, using capacitive stacks with printed graphene or encapsulated MXene and microstructured dielectrics, and readout by RC/CDC electronics for long-term baseline stability. (d) Self-powered touch interfaces, where triboelectric and hybrid tribo + piezo sensors with graphene or MXene electrodes generate event-driven pulses for touch-to-trigger interactions.

The wearable pulse/blood pressure (BP) monitoring system operates at extremely low external pressures with 1 Hz dynamic signals which makes graphene microcrack piezoresistive films the best choice for this application. Specifically, the sensors deliver high sensitivity below kPa levels while keeping their reference point stable and using little power and showing no performance degradation after running thousands of times. MXene aerogel sensors operate at low pressure detection levels which match or exceed graphene sensors but their stable operation needs protective coatings to prevent oxidation, which increases system complexity and drift potential. Thus, the main material for ultra-low-pressure dynamic pulse detection should be graphene because it provides stable baseline measurements and long-term durability. MXene sensors show potential for peak sensitivity applications but their stability remains limited so they should only be used when appropriate encapsulation methods are available. In summary, the wrist-pulse patch depends on graphene piezoresistive e-skin as its main sensor but users can add MXene elements through appropriate encapsulation methods to achieve better sensitivity when maintenance needs are not a concern (Fig. 8a).

- Tactile sensing in soft robotic fingers operates across a broad pressure range, starting at 1–10 kPa during initial contact and reaching 50–100 kPa when the finger grips an object. In

addition, the system needs to measure static loads and dynamic signals with high precision force measurement at sub-kPa levels and fast response times under 10 milliseconds while maintaining contact with flexible surfaces that stretch and curve. Furthermore, the system requires multiple grasp cycles before it needs to be replaced. MXene-based composites match the requirements of this regime because MXene/polymer nanofiber capacitive skins demonstrate linear behavior from 0 to 400 kPa and maintain their functionality through more than 10 000 cycles at pressures exceeding 167 kPa. Similarly, the MXene composite sensors demonstrate quick response times of 45–50 ms while operating within 0–200 kPa and enduring numerous cycles to detect both light and forceful grip applications.[133] Moreover, the combination of a MXene coating with porous elastomer foam or MXene–polymer nanofiber stacks produces a force sensor which shows stable quasi-linear performance with minimal drift throughout multiple cycles for accurate fingertip force measurement.[150]

Graphene shows promise for tactile e-skin and robotic fingertip applications because scientists can create it to detect both extremely light pressures and a broad range of pressures.[69] Specifically, the combination of microstructures and crack formation in graphene piezoresistive films enables them to detect small mechanical forces: a graphene-oxide design achieved 232.5 kPa^{-1} sensitivity within the 0–0.2 kPa range while maintaining 45 ms response time and continuous operation for pulse and first-touch applications.[34] Likewise, the capacitive microconformal graphene electrodes show high sensitivity because they can detect small signals within 30 ms, which makes them suitable for wearable health monitoring and tactile sensor development. Additionally, the system operates between 20 Pa and 1.4 MPa because it uses laser-induced graphene (LIG) with a microstructured TPU dielectric material which maintains flexibility and stability during more than 4000 operational cycles.[151] Similarly, the manufacturing process for ink-printed porous graphene sensors enables high-resolution measurements of less than 0.3 kPa across a 0.3 kPa–1 MPa range while showing stable repeated results, which makes them suitable for gait mapping, seating and gripper pad applications.[152] Overall, the flexible tactile system achieves high sensitivity and high loading capacity through the combination of microstructure optimization (cracks and domes) with electrode design (microconformal) and morphology selection (LIG and porous inks).

The MXene-based composites (foams or polymer–nanofiber capacitive skins) detect touch from light to firm grip through their near-linear response across the 0–200/400 kPa pressure range and 45–50 ms response time and excellent cycling stability which suits soft-robotic fingertip applications. Meanwhile, the piezoresistive films made from graphene operate in two separate modes which use crack-based sensitivity to detect first-touch and sub-kPa level pulses and capacitive formats with laser-induced graphene, and microstructured dielectrics achieve MPa range sensitivity with flexible and repeatable performance. Furthermore, the printed/porous graphene manufacturing process allows for affordable mass production of dense arrays with precise detail. Base material performance depends equally on the microstructure and electrode design and packaging methods. Therefore, the design should place MXene–textile or MXene–nanofiber stacks at the center of the load-bearing channel because they provide wide quasi-linear durability and thin protective encapsulation prevents oxidation. Additionally, the system requires a graphene piezoresistive or LIG capacitive layer to detect ultralow-pressure signals while maintaining long-term baseline stability. Thus, the design uses row/column capacitive scanning for arrays and includes small resistive MXene pads at high-load hotspots when needed. In summary, the system uses MXenes for extended range and durability, graphene for improved sensitivity and stability, and hybrid layering for applications needing both high and low performance levels (Fig. 8b).

- Wearable foot-pressure and gait insoles faced pressure changes between 5 and 10 kPa which happen during walking at 150–300 kPa peak forces.[83] In this regard, the sensor material MXene shows excellent compatibility with textile applications because CTS/MXene textile pressure sensors demonstrate 1.16 kPa^{-1} sensitivity and operate from 0 to 1.5 MPa with minimal degradation after 1000 loading cycles at 1.5 MPa. Furthermore, the capacitive insole design uses a MXene composite nanofibrous material with porous dielectrics (spacer fabric/foam) to achieve stable wide-range pressure measurement (up to 0–400 kPa), which enables low-power row/column scanning operations.[133] Accordingly, the design for this application requires capacitive arrays to be stacked with MXene foam pads placed at heel and toe positions for measuring single-point forces. However, the main drawback of MXene materials occurs when they experience oxidation during exposure to humid or sweaty conditions but polymer encapsulation and binder embedding help protect them from degradation. Therefore, the preferred solution for complete plantar surface mapping at low power consumption involves using a capacitive MXene–textile grid which needs a suitable protective coating. Overall, the capacitive MXene–textile grid achieves optimal results for complete plantar surface mapping while using minimal power but resistive MXene pads perform better for particular high-load areas.

The gait/foot insoles experience their highest operating forces between 150 and 300 kPa when walking but MXene textiles/composite nanofibers match the natural conditions of these forces. As a result, the materials show excellent performance in capacitive row/column mapping at low power consumption while maintaining their durability through multiple cycles. Yet, the main drawback of MXene materials occurs through environmental oxidation but researchers have developed two solutions to protect them: polymer encapsulation and binder embedding. In contrast, the main application of graphene involves its use as a stable printable electrode for capacitive stacks and its role in low-load areas but its piezoresistive films experience reliability issues when subjected to multiple hundreds-of-kPa compressions without

an additional structural support. Thus, the main application of MXenes in plantar mapping requires their ability to handle high loads and wide measurement ranges but graphene serves as a stable electrode material for capacitive applications. Consequently, the solution recommendation consists of a capacitive MXene–textile grid with a laminated sandwich construction, a porous dielectric material for main mapping operations and a thin protective coating for stability. Additionally, the system needs resistive MXene pads to be placed at heel and toe positions for force peak measurement and printed graphene electrodes for interconnected and auxiliary applications that require stability and patterning (Fig. 8b).

- Ultralow-power continuous monitor devices, such as external blood pressure cuffs/patches, involve tracking both steady and progressive pressure variations, which range from 0–20 kPa for seated load distribution and 0–16 kPa for external arterial loading. In addition, the sensor needs to operate at its lowest power consumption level while maintaining its calibration stability during extended operation and typical user activities.[153] In this context, the capacitive pressure sensor operates at zero DC power consumption because it uses capacitor charging and discharging times for measurement, which makes it suitable for ultra-low-power pressure monitoring.[154] MXene and graphene electrodes create flexible capacitive sensors according to the literature to validate their power advantages and operational characteristics. However, the long-term operation of battery-powered capacitive sensors benefits from graphene electrodes because graphene shows chemical stability and resists oxidation. The protective coatings or encapsulation of MXene electrodes help maintain their high conductivity but these materials require additional protection to prevent oxidation during use under humid or sweaty conditions.[155] Importantly, the slightly elevated sheet resistance of graphene electrodes does not impact capacitive sensing because the measurement system detects changes in capacitance values instead of series resistance values. The sensor detects low pressures through its ability to measure increased thickness variations which occur when graphene films are arranged across soft dielectric materials including PDMS microdomes and spacer elastomers.[73] By contrast, triboelectric generators have the potential to generate zero-power touch signals through motion detection but they produce no output when loads remain steady, so they are not suitable for continuous presence/pressure monitoring.[156] Therefore, the optimal solution for continuous operation of low-power wearable devices and furniture-mounted sensors requires graphene-based capacitive architectures with microstructured dielectrics but MXene-based capacitive electrodes function well when they receive suitable encapsulation for stability purposes.

The operating conditions of ultra-low-power continuous monitors (seat cushions and external BP cuffs/patches) occur in moderate static pressure ranges between 0 and 20 kPa for seating and 0 and 16 kPa for external arterial loading. As a result, the capacitive architecture works best for always-on applications because it enables duty-cycled resistor–capacitor (RC) readout with zero DC power consumption, and graphene electrodes with microstructured dielectrics (PDMS microdomes or spacer elastomers) achieve stable baselines and excellent low-pressure sensitivity because of graphene's chemical stability. The performance of MXene electrodes depends on suitable encapsulation methods which help protect them from oxidation-related drift during exposure to humid or sweaty conditions. Meanwhile, the event-driven operation of triboelectric devices prevents them from functioning as continuous presence/pressure monitors because they produce signals only when objects touch or separate but not when they experience steady pressure. Consequently, the recommended solution for continuous monitoring applications needs capacitive stacks with graphene electrodes and microstructured dielectrics to achieve stable long-term operation and detect low loads. The selection process for MXene electrodes in particular applications needs protection through barrier laminations and polymer binders and scheduled baseline verification. In summary, the proposed solution for steady-state presence sensing consists of a graphene-electrode capacitive sensor with a microstructured dielectric and low-duty-cycle RC readout as its core structure and MXene electrodes with protective encapsulation and scheduled baseline verification (Fig. 8c).

- Self-powered operation generates electrical power through touch-based interfaces that function as robotic e-skin or wearable buttons, producing voltage pulses upon contact.[157] In this context, the best options for this application include triboelectric sensors (triboelectric nanogenerators) and hybrid tribo/piezoelectric designs that use MXene or graphene electrodes.[158] For example, a triboelectric layer with a graphene electrode (*e.g.* laser-induced graphene on polyimide paired with a soft tribo-active silicone) functions as a flexible patterned self-powered touch pad which produces voltage spikes during each tap operation suitable for wearable keyboards and robot skin without batteries.[159] Moreover, the high surface charge density of MXenes enables effective electrode and tribo layer operation in TENGs which produce strong electrical signals but require protection against environmental oxidation. However, the high surface charge density of MXenes enhances output but the material becomes more susceptible to environmental oxidation when exposed to air.[160] By comparison, the combination of graphene with triboelectric interface technology shows promising long-term tactile skin performance but MXene hybrids produce superior signal amplitude results. Nevertheless, the main restriction of triboelectric sensors exists in their ability to detect only touch events and release actions but they fail to measure force intensity, so designers need to add static piezoresistive elements for force magnitude tracking. As a result, the graphene triboelectric patch operates as a thin self-powered touch trigger system for basic e-skin tile applications.

The system operates as an event-driven system because triboelectric interfaces generate contact-based voltage pulses instead of steady signals. Accordingly, the combination of graphene electrodes with LIG electrodes enables stable flexible operation for long periods, while MXene hybrids with suitable encapsulation methods produce enhanced output

amplitudes. Therefore, the system should use triboelectric sensing for touch detection, graphene electrodes for stability and MXene hybrids for peak signal requirements with protective barriers to maintain baseline performance. In summary, the system depends on a graphene-electrode TENG as its main touch interface for battery-less tactile pads and e-skin tiles but uses a static channel to measure force magnitude and MXenes with protective barriers to achieve maximum pulse amplitude under particular conditions (Fig. 8d). Summarizing the above in a simplified mapping:

1) Ultra-low pressure, dynamic signals (pulse, sound)

- Mechanism: piezoelectric or crack-mediated piezoresistive.
- Material/electrodes: graphene (laser-induced graphene or ultrathin cracked films).
- Architecture: thin graphene film on PDMS/Ecoflex with light microtexturing (*e.g.*, microdomes); secure mechanical mounting to reduce motion noise.
- Encapsulation: thin PDMS; add parylene-C or breathable PU for humid/sweaty use.
- Readout: piezo → charge amplifier (very high input impedance); piezoresistive → Wheatstone bridge + low-drift TIA/analog-to-digital converter (ADC).
- Notes: excellent sub-kPa sensitivity and waveform fidelity; narrower linear window and potential hysteresis at higher strain.

2) Wide-range, static or slowly varying load (soft robots, prosthetics, insoles)

- Mechanism: piezoresistive (percolating) or capacitive.
- Material/electrodes: MXene composites/textiles (with robust protection) or graphene electrodes for capacitive stacks.
- Architecture: conductive PU foam/aerogel (MXene) or microstructured capacitor with a soft dielectric; for textiles, interlocked/elastic weaves.
- Encapsulation: PDMS/PU moisture barrier with sealed edges; maintain breathability for wearables.
- Readout: resistive → precision bridge/ADC; capacitive → capacitance-to-digital converter (CDC) or RC-oscillator with thermal calibration.
- Notes: better linearity, high load tolerance, strong cycling endurance; MXenes require oxidation/humidity protection.

3) Continuous monitoring with minimal power (long-term wear)

- Mechanism: capacitive (near-zero bias current).
- Material/electrodes: printed/mesh graphene or well-encapsulated MXenes.
- Architecture: microstructured dielectric over flexible electrodes; matrix/row–column addressing if needed.
- Encapsulation: thin, breathable barrier; choose materials with low drift under sweat/temperature.
- Readout: low-power CDC with long-term baseline calibration.
- Notes: very stable baseline and ultra-low power; monitor and correct slow thermal/time drift.

4) Self-powered, sporadic sensing (touch triggers, energy-harvesting skins)

- Mechanism: triboelectric or hybrid tribo + piezo.
- Material/electrodes: graphene for stability; MXenes for boosted output if well protected.
- Architecture: micro-textured tribo surfaces (hierarchical ridges/dimples) or frictional textiles; include rectification and storage.
- Encapsulation: moisture protection for MXenes; durable contact layers to limit wear.
- Readout: rectifier + storage capacitor with high-impedance front end; add charge amp for the piezo channel in hybrids.
- Notes: great for event-driven triggers and touch; not ideal for purely static measurements without integration algorithms.

7.2 Manufacturability and scalability considerations

The selection of materials depends on how manufacturers can produce and scale the sensor devices. Overall, the production of graphene-based sensors has reached maturity because researchers can use screen and inkjet printing to create solution-processed graphene and rGO inks from exfoliated graphite for making it possible to create pressure sensors on flexible substrates.[152] The production of high-quality monolayer graphene through CVD methods results in excellent results for skin patch applications but the process faces difficulties when attempting to scale up production through roll-to-roll methods because of defect formation during transfer processes.[161] However, the production of MXene materials remains less advanced than other materials because it needs to extract MAX phases through chemical etching followed by delamination to obtain conductive flakes which can be transformed into printable inks.[162] The production of MXene materials requires dangerous chemicals for processing, while the resulting ink solutions lose their conductivity within short time periods unless stored under protective conditions, which creates difficulties for mass production of stable products.[18] The stability of graphene inks exceeds that of MXene inks because graphene inks maintain their conductivity during storage and they integrate seamlessly with current printing and flexible circuit manufacturing systems.[155] The production costs of graphene remain affordable because graphite exists abundantly while MXenes face higher expenses because of their complex manufacturing process, limited yield and handling difficulties.[163] The integration process for low-cost readout electronics with graphene and MXene electrodes requires basic steps for resistive and capacitive mechanisms but piezoelectric/triboelectric modes require advanced front-end electronics and precise packaging techniques.[164,165] Consequently, the current market for wearable products uses graphene-based pressure sensors because they offer stable performance, printability and availability but MXene sensors are developed for specific high-performance applications that need extreme pressure sensitivity and enhanced durability.[18]

8. Challenges, open questions, and future directions

The current state-of-the-art analysis has been completed through a design framework evaluation to identify ongoing difficulties

that affect MXene and graphene flexible pressure sensors. The development of flexible pressure sensors faces multiple obstacles which include material degradation, hysteresis effects, testing standardization, integration complexities and opportunities for multi-functional sensing skin development.

8.1 Material-level challenges: stability and reliability

The reliability of MXene and graphene materials depends on their specific properties which determine their performance in actual applications. In particular, MXene stability faces its primary challenge because the material transforms into TiO_2 when it encounters oxygen and moisture, which results in resistance growth and baseline shift and complete device failure during prolonged operation in hot or damp environments or when used on human skin. The protection of MXene flakes through matrix embedding and surface modification and polymer encapsulation methods extends their operational life but researchers continue to develop methods for commercial applications that achieve stable calibration over long periods.[18,120] Conversely, the chemical stability of graphene remains excellent from a chemical standpoint but its mechanical properties lead to unreliable performance. The majority of high-sensitivity graphene piezoresistive sensors depend on engineered microcracks which expand during multiple loading cycles to produce significant hysteresis effects and baseline shifts and eventually lead to film failure through tearing.[166] The implementation of preconditioning techniques alongside composite structures containing elastic matrices with graphene and software-based compensation helps minimize but does not eliminate the problem, so researchers select foam and textile materials instead of thin brittle films for their designs.[167] The development of flexible MXene and graphene sensors continues to face challenges because of their inconsistent measurement outcomes. The combination of engineered microstructures with advanced process control systems leads to better environmental stability when performing repeated loading tests under harsh conditions.[60,168] The packaging process needs careful handling because MXene materials become oxidized during hot lamination and graphene materials lose contact with soft silicones because of their weak interface bonds. Therefore, the development of new sealing techniques together with improved interface materials represents a critical requirement for sensor stability and biocompatibility maintenance during real-world operations.[120,169]

8.2 Measurement standardization and comparability

MXene/graphene pressure sensors with flexible design produce inconsistent results which make it impossible to compare their findings because the field requires established testing protocols that specify evaluation methods and common criteria for assessing dynamic performance and durability. Therefore, standardized testing protocols and reporting metrics are required to enable fair and objective comparison between different MXene- and graphene-based pressure sensing systems. Specifically, the field needs a standardized testing system which consists of three fundamental elements: (i) sensitivity evaluation through two pressure ranges (low to high) with established normalization to ΔSignal/ΔPressure using kPa or $\Delta C/C_0$ per kPa units, (ii) execution of a standardized load sequence with stepwise pressure increments to maximum load and recording of loading and unloading curves, and (iii) calculation of the average slope, hysteresis and limit of detection as the smallest pressure that produces a signal greater than three times the noise level. The testing protocol requires either a small-amplitude oscillation test or a defined step input to determine dynamic response times during the rise and recovery phases. The durability test consists of 1000 load cycles at 50% of the full-scale range to determine the amount of signal degradation. Moreover, the results should present statistical data from multiple devices through mean values and standard deviations instead of showing results from a single sensor. The sensor needs to show its operational readiness through output stability measurements that occur when it experiences different bending radii and temperature variations. The development of test standards for these sensors requires simultaneous work with system integration problems which affect their ability to transition from laboratory settings. The majority of MXene/graphene sensors operate through resistance or capacitance measurements which require precise bonding to small readout/battery/wireless modules without introducing stress points that would separate the sensor from its substrate or distort its signal output. The development of stretchable wiring with printed conductive inks based on MXene/graphene materials solves the need for reliable strain-relief geometries. The signal processing needs for arrays require real-time force pattern analysis through machine learning-based methods or onboard processing systems that operate at low power levels. The packaging requirements for long-term wearability need to protect MXene materials from moisture while using skin-friendly materials that allow for breathability. The process to obtain direct skin contact approval requires MXene/PVA film cytotoxicity testing and evidence that cells can grow during short exposure times. Finally, real product development needs ultralow-power readout systems and Bluetooth/NFC connectivity or energy harvesting capabilities because triboelectric/piezo harvesters generate only supplemental power which is insufficient to run monitoring systems independently. The development of e-skins for multimodal sensing requires researchers to solve the challenge of separating and deconvolving signals from different measurement types including pressure, strain and temperature. The development of these sensors requires better materials, established testing protocols and system integration techniques which will achieve both power efficiency and biocompatibility.

8.3 Toward multimodal electronic skin

The development of e-skin requires a flexible sheet which detects multiple stimuli including pressure, strain, temperature, humidity and biochemical signals similar to human skin. In

this context, the development of e-skin requires MXenes and graphene as fundamental materials because they can be arranged into patterns and stacked onto flexible substrates.[170] The main difficulty in achieving simultaneous strain and pressure measurement requires developers to separate normal force measurements from stretching and bending effects.

For this purpose, the combination of a MXene piezoresistive foam for normal pressure detection and a graphene serpentine strain gauge for in-plane stretching measurement represents a solution for dual-mode strain and pressure detection. The combination of graphene for strain detection and MXene for pressure detection through vertical layer placement represents a solution for dual-mode strain and pressure detection. As illustrated in Fig. 9, a representative layered e-skin architecture places a MXene foam, a graphene serpentine, and a thermistor element on separate sensing islands above a microfluidic/skin interface, enabling clean spatial and functional decoupling of pressure, strain, and temperature signals. The dual-mode MXene fiber concepts operate through one thread which allows pressure and strain measurement through independent channels.[162] The temperature sensitivity of MXene and graphene materials allows developers to create separate thermistor layers which measure temperature while using pressure sensors that remain insensitive to temperature changes.[171] In one configuration, the system uses a MXene aerogel channel to measure pressure and temperature signals which are then subtracted from a temperature-only reference channel to extract pressure data. The integration of chemical and biosensing functions in e-skin systems becomes possible through the use of graphene field-effect transistor-style elements and functionalized MXene electrodes which detect gases and sweat. The main challenge for e-skin development involves packaging because sweat and humidity which benefit chemical detection create problems for mechanical signal measurement. The use of e-skin technology enables controlled transport of sweat toward dedicated graphene/MXene chemo-sensing regions through integrated microfluidic channels, while maintaining dry and stable pressure-sensing pixels.[18] The transparent and conductive properties of graphene allow developers to make stretchable electrodes for optoelectronic pixels and high-sensitivity pressure films which enable skins to detect touch and guide or emit light.[172] The combination of MXenes' excellent conductivity and electromagnetic interference (EMI) shielding properties makes them suitable for use as ground/shield layers which protect graphene sensing/display layers from electromagnetic interference in dense wearable systems.[162] Looking ahead, the future e-skin technology will combine MXenes with graphene because MXenes offer strong conductive elements and multiple sensing functions and graphene provides sensitive stretchable and optically transparent properties.[162] The development of this concept requires developers to create system-level signal processing solutions which will enable them to separate different stimuli through mathematical processing of combined channel data. To achieve pure pressure or strain measurements, biological skin signals can be processed using multiple sensor channels combined with lightweight calibration models or machine learning algorithms. Consequently, the engineering community supports deterministic decoupling methods which use separate geometries, stacked layers and isolated channels because these approaches simplify calibration processes and enhance device reliability in real-world applications.

9. Conclusion

Flexible pressure sensors made from MXene and graphene materials benefit from their individual performance characteristics. Specifically, the sub-kPa pressure range sensitivity of graphene crack-network films makes them suitable for detecting micro-physiological signals and delicate tactile information, while MXene composites, aerogels and textiles provide quasi-linear responses and electrical continuity from tens to hundreds of kPa with excellent cycling performance. Thus, the system achieves its complementary performance through its network structure which uses junction-level crack modulation and progressive densification of percolating networks. The design process becomes simple because graphene works best for small pressure measurements and light loads, while MXenes operate better under heavy loads, extensive pressure ranges and prolonged operation.

The development of new materials faces specific obstacles which stem from their individual properties. For MXenes, the baseline stability of MXenes requires protective matrices or sealed systems to prevent oxygen and moisture damage when

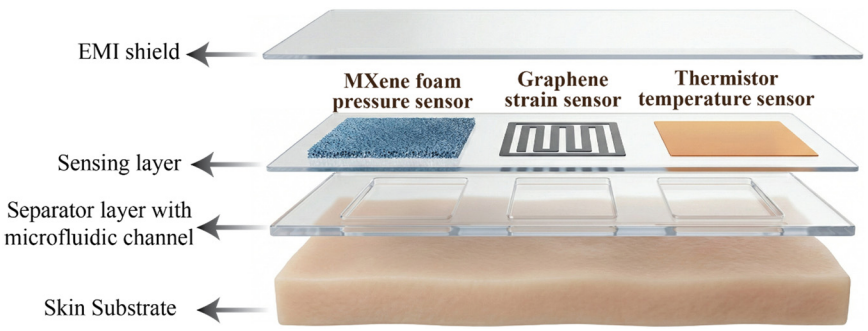

Fig. 9 Layered architecture for multimodal e-skin showing independent MXene-based pressure sensing, graphene serpentine strain sensing, and thermistor-based temperature sensing, each isolated on separate islands to enable clean signal decoupling.

used for on-skin applications. For graphene, the high-gain crack mechanisms of graphene require microstructural control or supportive substrates or hybrid fillers to achieve improved cycling performance and decreased hysteresis and drift. The development of standard packaging methods and improved process control systems will help solve the common problems of device reproducibility and packaging.

The researchers require standardized testing methods to achieve equal device evaluation while industrial organizations need established evaluation protocols to validate their products. Accordingly, organizations must perform multiple pressure window sensitivity tests under standardized load sequences which include full loading and unloading data and precise hysteresis and drift measurements and durability statistics for multiple devices. Standardized testing methods enable scientists to identify universal design solutions because they remove false test results from the analysis.

The future development of graphene electrode printing technology and MXene ink stability improvements and roll-to-roll processing advancements will determine manufacturing capabilities. In parallel, the development of hybrid sensor stacks which unite static resistive and capacitive channels with dynamic piezo and tribo channels will allow sophisticated low-power e-skins to be built. The future development of multimodal e-skins will depend on MXenes for their ability to conduct electricity and detect pressure and temperature while shielding from electromagnetic interference, while graphene will be used for its exceptional sensitivity and stretchability and optical properties. Finally, the development of test standards, packaging solutions and low-power reading systems needs to match the current advancements in materials science.

Conflicts of interest

There are no conflicts to declare.

Data availability

No new experimental data were generated or analyzed in this study. All data discussed are derived from previously published literature.

References

1 X. Chen, C. Wang, W. Wei, Y. Liu, S. S. Ge, L. Zhou and H. Kong, Flexible and Sensitive Pressure Sensor with Enhanced Breathability for Advanced Wearable Health Monitoring, *npj Flexible Electron.*, 2025, **9**, 101, DOI: 10.1038/s41528-025-00469-6.
2 S. Wang, H. Zhai, Q. Zhang, X. Hu, Y. Li, X. Xiong, R. Ma, J. Wang, Y. Chang and L. Wu, Trends in Flexible Sensing Technology in Smart Wearable Mechanisms–Materials–Applications, *Nanomaterials*, 2025, **15**, 298, DOI: 10.3390/nano15040298.
3 M. Nabeel, M. Mousa, B. Viskolcz, B. Fiser and L. Vanyorek, Recent Advances in Flexible Foam Pressure Sensors: Manufacturing, Characterization, and Applications – a Review, *Polym. Rev.*, 2023, 1–41, DOI: 10.1080/15583724.2023.2262558.
4 M. Nabeel, A. J. Addie, B. Viskolcz, M. Kollar, B. Fiser and L. Vanyorek, Integrating Polyurethane-silicone Rubber-nanohybrid Systems for Improved Wearable Pressure Sensing, *Polym. Compos.*, 2025, **46**, 169–182, DOI: 10.1002/pc.28976.
5 Y. Gu, Y. Luo, Q. Guo, W. Yu, P. Li, X. Wang, T. Ye, H. Chang, W. Yuan and H. Wu, *et al.*, Empowering Human-Machine Interfaces: Self-Powered Hydrogel Sensors for Flexible and Intelligent Systems, *Adv. Funct. Mater.*, 2025, e09085, DOI: 10.1002/adfm.202509085.
6 R. Qin, J. Nong, K. Wang, Y. Liu, S. Zhou, M. Hu, H. Zhao and G. Shan, Recent Advances in Flexible Pressure Sensors Based on MXene Materials, *Adv. Mater.*, 2024, **36**, 2312761, DOI: 10.1002/adma.202312761.
7 Z. Zhang, Q. Liu, H. Ma, N. Ke, J. Ding, W. Zhang and X. Fan, Recent Advances in Graphene-Based Pressure Sensors: A Review, *IEEE Sens. J.*, 2024, **24**, 25227–25248, DOI: 10.1109/JSEN.2024.3419243.
8 C. I. Idumah, Influence of Surfaces and Interfaces on MXene and MXene Hybrid Polymeric Nanoarchitectures, Properties, and Applications, *J. Mater. Sci.*, 2022, **57**, 14579–14619, DOI: 10.1007/s10853-022-07526-9.
9 Y. Zhou, H. Lian, Z. Li, L. Yin, Q. Ji, K. Li, F. Qi and Y. Huang, Crack Engineering Boosts the Performance of Flexible Sensors, *VIEW*, 2022, **3**(5), 1–26, DOI: 10.1002/VIW.20220025.
10 L. Zhang, R. Bao and C. Pan, Recent Advances and Current Challenges of High-Sensitivity Resistive Pressure Sensors for Position Recognition, *J. Phys. Chem. Lett.*, 2025, **16**, 9169–9182, DOI: 10.1021/acs.jpclett.5c01566.
11 P. Li, L. Zhao, Z. Jiang, M. Yu, Z. Li, X. Zhou and Y. Zhao, A Wearable and Sensitive Graphene-Cotton Based Pressure Sensor for Human Physiological Signals Monitoring, *Sci. Rep.*, 2019, **9**, 14457, DOI: 10.1038/s41598-019-50997-1.
12 T. Mukherjee and D. Gupta, Cognitive Gripping with Flexible Graphene Printed Multi-Sensor Array, *Commun. Eng.*, 2023, **2**, 57, DOI: 10.1038/s44172-023-00095-y.
13 T. Chen, Z. Liu, G. Zhao, Z. Qin, P. Zheng, J. T. Aladejana, Z. Tang, M. Weng, X. Peng and J. Chang, Piezoresistive Sensor Containing Lamellar MXene-Plant Fiber Sponge Obtained with Aqueous MXene Ink, *ACS Appl. Mater. Interfaces*, 2022, **14**, 51361–51372, DOI: 10.1021/acsami.2c15922.
14 L. P. Yu, X. H. Zhou, L. Lu, L. Xu and F. J. Wang, MXene/Carbon Nanotube Hybrids: Synthesis, Structures, Properties, and Applications, *ChemSusChem*, 2021, **14**, 5079–5111, DOI: 10.1002/cssc.202101614.
15 Y. Luo, M. R. Abidian, J.-H. Ahn, D. Akinwande, A. M. Andrews, M. Antonietti, Z. Bao, M. Berggren, C. A. Berkey and C. J. Bettinger, *et al.*, Technology Roadmap for Flexible Sensors, *ACS Nano*, 2023, **17**, 5211–5295, DOI: 10.1021/acsnano.2c12606.
16 T. Habib, X. Zhao, S. A. Shah, Y. Chen, W. Sun, H. An, J. L. Lutkenhaus, M. Radovic and M. J. Green, Oxidation Stability of $Ti_3C_2T_x$ MXene Nanosheets in Solvents and Composite Films, *npj 2D Mater. Appl.*, 2019, **3**, 8, DOI: 10.1038/s41699-019-0089-3.

17 N. Kim, D. Yun, I. Hwang, G. Yoon, S. M. Kang and Y. W. Choi, Crack-Based Sensor with Microstructures for Strain and Pressure Sensing, *Sensors*, 2023, **23**, 5545, DOI: 10.3390/s23125545.

18 Y. Yao, X. Li, K. M. Sisican, R. M. C. Ramos, M. Judicpa, S. Qin, J. Zhang, J. Yao, J. M. Razal and K. A. S. Usman, Progress towards Efficient MXene Sensors, *Commun. Mater.*, 2025, **6**, 210, DOI: 10.1038/s43246-025-00907-y.

19 S. Nouseen and M. Pumera, Electrochemical Etching of MXenes: Mechanism, Challenges and Future Outlooks, *J. Mater. Chem. A*, 2025, **13**, 34055–34084, DOI: 10.1039/D5TA04176G.

20 J. A. Adorna, V. D. Dang, V. T. Nguyen, B. K. Nahak, K.-K. Liu and R.-A. Doong, Functionalization of MXenes [Ti_3C_2(=O/OH/F)X] with Highly Mesoporous NH_2-Activated Biochar for Permselective Salty Ions Removal by Capacitive Deionization, *Chem. Eng. J.*, 2025, **504**, 158802, DOI: 10.1016/j.cej.2024.158802.

21 S. Abdolhosseinzadeh, M. Jafarpour, J. Heier, F. Nüesch and C. Zhang, Solution Processing of MXenes for Printing, Wet Coating, and 2D Film Formation, in *Transition Metal Carbides and Nitrides (MXenes) Handbook*, Wiley, 2024, pp. 272–293.

22 R. Liu and W. Li, High-Thermal-Stability and High-Thermal-Conductivity $Ti_3C_2T_x$ MXene/Poly(Vinyl Alcohol) (PVA) Composites, *ACS Omega*, 2018, **3**, 2609–2617, DOI: 10.1021/acsomega.7b02001.

23 H. Zhang, C. Du and Y. Zhang, Constructing the 3D Interconnected Conductive MXene-Cellulose Scaffold to Boosting the Piezoresistive Sensing Capability, *ACS Appl. Electron. Mater.*, 2024, **6**, 6785–6792, DOI: 10.1021/acsaelm.4c01187.

24 X.-H. Zhang, B. Wang, B. Zhou, H.-J. Lin, Y.-X. Liu, F.-M. Yang, S.-K. Sun, Q.-H. Song and Q. Wu, Recent Advances in MXene-Based Flexible Pressure Sensors for Medical Monitoring, *Rare Met.*, 2025, **44**, 3653–3685, DOI: 10.1007/s12598-024-03157-y.

25 R. A. Soomro, P. Zhang, B. Fan, Y. Wei and B. Xu, Progression in the Oxidation Stability of MXenes, *Nano-Micro Lett.*, 2023, **15**, 108, DOI: 10.1007/s40820-023-01069-7.

26 T. Su, C. Rong, T. Yu, S. Hu, P. He, B. Zhang, Y. Yan and F.-Z. Xuan, Progress and Perspectives of High-Quality Mechanical Properties Testing and Mechanisms for 2D Materials, *Int. J. Extreme Manuf.*, 2026, **8**, 012002, DOI: 10.1088/2631-7990/ae0216.

27 Y. Wang, Y. Yue, F. Cheng, Y. Cheng, B. Ge, N. Liu and Y. Gao, $Ti_3C_2T_x$ MXene-Based Flexible Piezoresistive Physical Sensors, *ACS Nano*, 2022, **16**, 1734–1758, DOI: 10.1021/acsnano.1c09925.

28 Z. Wu, T. Shang, Y. Deng, Y. Tao and Q. Yang, The Assembly of MXenes from 2D to 3D, *Adv. Sci.*, 2020, **7**(7), DOI: 10.1002/advs.201903077.

29 X. Shi, H. Wang, X. Xie, Q. Xue, J. Zhang, S. Kang, C. Wang, J. Liang and Y. Chen, Bioinspired Ultrasensitive and Stretchable MXene-Based Strain Sensor via Nacre-Mimetic Microscale "Brick-and-Mortar" Architecture, *ACS Nano*, 2019, **13**, 649–659, DOI: 10.1021/acsnano.8b07805.

30 R. Qin, X. Li, M. Hu, G. Shan, R. Seeram and M. Yin, Preparation of High-Performance MXene/PVA-Based Flexible Pressure Sensors with Adjustable Sensitivity and Sensing Range, *Sens. Actuators, A*, 2022, **338**, 113458, DOI: 10.1016/j.sna.2022.113458.

31 X.-P. Li, Y. Li, X. Li, D. Song, P. Min, C. Hu, H.-B. Zhang, N. Koratkar and Z.-Z. Yu, Highly Sensitive, Reliable and Flexible Piezoresistive Pressure Sensors Featuring Polyurethane Sponge Coated with MXene Sheets, *J. Colloid Interface Sci.*, 2019, **542**, 54–62, DOI: 10.1016/j.jcis.2019.01.123.

32 A. VahidMohammadi, J. Rosen and Y. Gogotsi, The World of Two-Dimensional Carbides and Nitrides (MXenes), *Science*, 2021, **372**(6547), DOI: 10.1126/science.abf1581.

33 V. B. Mbayachi, E. Ndayiragije, T. Sammani, S. Taj, E. R. Mbuta and A. Ullah Khan, Graphene Synthesis, Characterization and Its Applications: A Review, *Results Chem.*, 2021, **3**, DOI: 10.1016/j.rechem.2021.100163.

34 J. Yang, S. Luo, X. Zhou, J. Li, J. Fu, W. Yang and D. Wei, Flexible, Tunable, and Ultrasensitive Capacitive Pressure Sensor with Microconformal Graphene Electrodes, *ACS Appl. Mater. Interfaces*, 2019, **11**, 14997–15006, DOI: 10.1021/acsami.9b02049.

35 A. Kaidarova, M. A. Khan, M. Marengo, L. Swanepoel, A. Przybysz, C. Muller, A. Fahlman, U. Buttner, N. R. Geraldi and R. P. Wilson, *et al.*, Wearable Multifunctional Printed Graphene Sensors, *npj Flexible Electron.*, 2019, **3**, 15, DOI: 10.1038/s41528-019-0061-5.

36 Z. Chen, W. Ren, L. Gao, B. Liu, S. Pei and H.-M. Cheng, Three-Dimensional Flexible and Conductive Interconnected Graphene Networks Grown by Chemical Vapour Deposition, *Nat. Mater.*, 2011, **10**, 424–428, DOI: 10.1038/nmat3001.

37 W. Yang and C. Wang, Graphene and the Related Conductive Inks for Flexible Electronics, *J. Mater. Chem. C*, 2016, **4**, 7193–7207, DOI: 10.1039/C6TC01625A.

38 Z. Hatab, A. Abdi, G. Steinbauer, M. E. Gadringer and W. Bösch, Propagation Constant Measurement Based on a Single Transmission Line Standard Using a Two-Port VNA, *Sensors*, 2023, **23**, 4548, DOI: 10.3390/s23094548.

39 H. Kou, L. Zhang, Q. Tan, G. Liu, H. Dong, W. Zhang and J. Xiong, Wireless Wide-Range Pressure Sensor Based on Graphene/PDMS Sponge for Tactile Monitoring, *Sci. Rep.*, 2019, **9**, 3916, DOI: 10.1038/s41598-019-40828-8.

40 L. Cheng, R. Wang, X. Hao and G. Liu, Design of Flexible Pressure Sensor Based on Conical Microstructure PDMS-Bilayer Graphene, *Sensors*, 2021, **21**, 289, DOI: 10.3390/s21010289.

41 E. Caffrey, J. R. Garcia, D. O'Suilleabhain, C. Gabbett, T. Carey and J. N. Coleman, Quantifying the Piezoresistive Mechanism in High-Performance Printed Graphene Strain Sensors, *ACS Appl. Mater. Interfaces*, 2022, **14**, 7141–7151, DOI: 10.1021/acsami.1c21623.

42 J. Wang, L. Sun, M. Zou, W. Gao, C. Liu, L. Shang, Z. Gu and Y. Zhao, Bioinspired Shape-Memory Graphene Film with Tunable Wettability, *Sci. Adv.*, 2017, **3**(6), DOI: 10.1126/sciadv.1700004.

43 Z. Shi, L. Meng, X. Shi, H. Li, J. Zhang, Q. Sun, X. Liu, J. Chen and S. Liu, Morphological Engineering of Sensing Materials for Flexible Pressure Sensors and Artificial Intelligence Applications, *Nano-Micro Lett.*, 2022, **14**, 141, DOI: 10.1007/s40820-022-00874-w.

44 R. Yang, A. Dutta, B. Li, N. Tiwari, W. Zhang, Z. Niu, Y. Gao, D. Erdely, X. Xin and T. Li, *et al.*, Iontronic Pressure Sensor with High Sensitivity over Ultra-Broad Linear Range Enabled by Laser-Induced Gradient Micro-Pyramids, *Nat. Commun.*, 2023, **14**, 2907, DOI: 10.1038/s41467-023-38274-2.

45 K. Manibalan and J.-T. Chen, Recent Progress on MXene–Polymer Composites for Soft Electronics Applications in Sensing and Biosensing: A Review, *J. Mater. Chem. A*, 2024, **12**, 27130–27156, DOI: 10.1039/D4TA04211E.

46 Z. Cai, M. Xu, X. Li, W. Liu, H. Yu and M. Yuan, High-Performance Wearable Pressure Sensor Based on Ag Nanowire/MXene Composite for Motion Monitoring, *Mater. Today Sustain.*, 2025, **31**, 101214, DOI: 10.1016/j.mtsust.2025.101214.

47 S. Zhang, F. Guo, X. Gao, M. Yang, X. Huang, D. Zhang, X. Li, Y. Zhang, Y. Shang and A. Cao, High-Strength, Antiswelling Directional Layered PVA/MXene Hydrogel for Wearable Devices and Underwater Sensing, *Adv. Sci.*, 2024, **11**(39), DOI: 10.1002/advs.202405880.

48 Y. Zhang, Y. Hu, P. Zhu, F. Han, Y. Zhu, R. Sun and C.-P. Wong, Flexible and Highly Sensitive Pressure Sensor Based on Microdome-Patterned PDMS Forming with Assistance of Colloid Self-Assembly and Replica Technique for Wearable Electronics, *ACS Appl. Mater. Interfaces*, 2017, **9**, 35968–35976, DOI: 10.1021/acsami.7b09617.

49 H. Xia, L. Wang, H. Zhang, Z. Wang, L. Zhu, H. Cai, Y. Ma, Z. Yang and D. Zhang, MXene/PPy@PDMS Sponge-Based Flexible Pressure Sensor for Human Posture Recognition with the Assistance of a Convolutional Neural Network in Deep Learning, *Microsyst. Nanoeng.*, 2023, **9**, 155, DOI: 10.1038/s41378-023-00605-0.

50 Y. Cai, J. Shen, C.-W. Yang, Y. Wan, H.-L. Tang, A. A. Aljarb, C. Chen, J.-H. Fu, X. Wei and K.-W. Huang, *et al.*, Mixed-Dimensional MXene-Hydrogel Heterostructures for Electronic Skin Sensors with Ultrabroad Working Range, *Sci. Adv.*, 2020, **6**(48), DOI: 10.1126/sciadv.abb5367.

51 R. Li, S. Chang, J. Bi, H. Guo, J. Yi and C. Chu, Flexible, Stretchable, and Self-Healing MXene-Based Conductive Hydrogels for Human Health Monitoring, *Polymers*, 2025, **17**, 2683, DOI: 10.3390/polym17192683.

52 Z. Luo, X. Hu, X. Tian, C. Luo, H. Xu, Q. Li, Q. Li, J. Zhang, F. Qiao and X. Wu, *et al.*, Structure-Property Relationships in Graphene-Based Strain and Pressure Sensors for Potential Artificial Intelligence Applications, *Sensors*, 2019, **19**, 1250, DOI: 10.3390/s19051250.

53 W. Zhu, Q. Wang, P. Zhang, L. Li, L. Zhang, H. Li, L. Ding, Z. Jin, P. Li and J. Zhang, The Functional Graphene/Epoxy Resin Composites Prepared by Novel Two-Phase Extraction towards Enhancing Mechanical Properties and Thermal Stability, *Front. Chem.*, 2024, **12**, DOI: 10.3389/fchem.2024.1433727.

54 M. Jin, W. Chen, L.-X. Liu, H.-B. Zhang, L. Ye, P. Min and Z.-Z. Yu, Transparent, Conductive and Flexible MXene Grid/Silver Nanowire Hierarchical Films for High-Performance Electromagnetic Interference Shielding, *J. Mater. Chem. A*, 2022, **10**, 14364–14373, DOI: 10.1039/D2TA03689D.

55 E. Gibertini, F. Lissandrello, L. Bertoli, P. Viviani and L. Magagnin, All-Inkjet-Printed Ti_3C_2 MXene Capacitor for Textile Energy Storage, *Coatings*, 2023, **13**, 230, DOI: 10.3390/coatings13020230.

56 S. Seyedin, S. Uzun, A. Levitt, B. Anasori, G. Dion, Y. Gogotsi and J. M. Razal, MXene Composite and Coaxial Fibers with High Stretchability and Conductivity for Wearable Strain Sensing Textiles, *Adv. Funct. Mater.*, 2020, **30**(12), DOI: 10.1002/adfm.201910504.

57 J. Zhang, K. Gao, S. Weng and H. Zhu, Graphene Nanoplatelets/Polydimethylsiloxane Flexible Strain Sensor with Improved Sandwich Structure, *Sensors*, 2024, **24**, 2856, DOI: 10.3390/s24092856.

58 Y. Cheng, Y. Xie, Z. Liu, S. Yan, Y. Ma, Y. Yue, J. Wang, Y. Gao and L. Li, Maximizing Electron Channels Enabled by MXene Aerogel for High-Performance Self-Healable Flexible Electronic Skin, *ACS Nano*, 2023, **17**, 1393–1402, DOI: 10.1021/acsnano.2c09933.

59 Y. Xiong, Y. Shen, L. Tian, Y. Hu, P. Zhu, R. Sun and C.-P. Wong, A Flexible, Ultra-Highly Sensitive and Stable Capacitive Pressure Sensor with Convex Microarrays for Motion and Health Monitoring, *Nano Energy*, 2020, **70**, 104436, DOI: 10.1016/j.nanoen.2019.104436.

60 Y. Zhang, J. Yang, X. Hou, G. Li, L. Wang, N. Bai, M. Cai, L. Zhao, Y. Wang and J. Zhang, *et al.*, Highly Stable Flexible Pressure Sensors with a Quasi-Homogeneous Composition and Interlinked Interfaces, *Nat. Commun.*, 2022, **13**, 1317, DOI: 10.1038/s41467-022-29093-y.

61 Y. Shi, X. Lü, J. Zhao, W. Wang, X. Meng, P. Wang and F. Li, Flexible Capacitive Pressure Sensor Based on Microstructured Composite Dielectric Layer for Broad Linear Range Pressure Sensing Applications, *Micromachines*, 2022, **13**, 223, DOI: 10.3390/mi13020223.

62 D. Jiang, J. Zhang, S. Qin, Z. Wang, K. A. S. Usman, D. Hegh, J. Liu, W. Lei and J. M. Razal, Superelastic $Ti_3C_2T_x$ MXene-Based Hybrid Aerogels for Compression-Resilient Devices, *ACS Nano*, 2021, **15**, 5000–5010, DOI: 10.1021/acsnano.0c09959.

63 M. Gu, X. Zhou, J. Shen, R. Xie, Y. Su, J. Gao, B. Zhao, J. Li, Y. Duan and Z. Wang, *et al.*, High-Sensitivity, Ultrawide Linear Range, Antibacterial Textile Pressure Sensor Based on Chitosan/MXene Hierarchical Architecture, *iScience*, 2024, **27**, 109481, DOI: 10.1016/j.isci.2024.109481.

64 H. Tian, Y. Shu, X.-F. Wang, M. A. Mohammad, Z. Bie, Q.-Y. Xie, C. Li, W.-T. Mi, Y. Yang and T.-L. Ren, A Graphene-Based Resistive Pressure Sensor with Record-High Sensitivity in a Wide Pressure Range, *Sci. Rep.*, 2015, **5**, 8603, DOI: 10.1038/srep08603.

65 Z. Hu, F. Xie, Y. Yan, H. Lu, J. Cheng, X. Liu and J. Li, Research Progress of Flexible Pressure Sensor Based on

MXene Materials, *RSC Adv.*, 2024, **14**, 9547–9558, DOI: 10.1039/D3RA07772A.

66 B. Shao, X. Chen, X. Chen, S. Peng and M. Song, Advancements in MXene Composite Materials for Wearable Sensors: A Review, *Sensors*, 2024, **24**, 4092, DOI: 10.3390/s24134092.

67 S. Hajian, D. Maddipatla, B. B. Narakathu and M. Z. Atashbar, MXene-Based Flexible Sensors: A Review, *Front. Sens.*, 2022, **3**, DOI: 10.3389/fsens.2022.1006749.

68 N. Liu, Q. Li, H. Wan, L. Chang, H. Wang, J. Fang, T. Ding, Q. Wen, L. Zhou and X. Xiao, High-Temperature Stability in Air of $Ti_3C_2T_x$ MXene-Based Composite with Extracted Bentonite, *Nat. Commun.*, 2022, **13**, 5551, DOI: 10.1038/s41467-022-33280-2.

69 R. Li, J. Hu, Y. Li, Y. Huang, L. Wang, M. Huang, Z. Wang, J. Chen, Y. Fan and L. Chen, Graphene-Based, Flexible, Wearable Piezoresistive Sensors with High Sensitivity for Tiny Pressure Detection, *Sensors*, 2025, **25**, 423, DOI: 10.3390/s25020423.

70 B. Lv, X. Chen and C. Liu, A Highly Sensitive Piezoresistive Pressure Sensor Based on Graphene Oxide/Polypyrrole@Polyurethane Sponge, *Sensors*, 2020, **20**, 1219, DOI: 10.3390/s20041219.

71 M. Su, P. Li, X. Liu, D. Wei and J. Yang, Textile-Based Flexible Capacitive Pressure Sensors: A Review, *Nanomaterials*, 2022, **12**, 1495, DOI: 10.3390/nano12091495.

72 X. He, Z. Liu, G. Shen, X. He, J. Liang, Y. Zhong, T. Liang, J. He, Y. Xin and C. Zhang, *et al.*, Microstructured Capacitive Sensor with Broad Detection Range and Long-Term Stability for Human Activity Detection, *npj Flexible Electron.*, 2021, **5**, 17, DOI: 10.1038/s41528-021-00114-y.

73 K. Zhao, J. Han, Y. Ma, Z. Tong, J. Suhr, M. Wang, L. Xiao, S. Jia and X. Chen, Highly Sensitive and Flexible Capacitive Pressure Sensors Based on Vertical Graphene and Micro-Pyramidal Dielectric Layer, *Nanomaterials*, 2023, **13**, 701, DOI: 10.3390/nano13040701.

74 J. Qian, R. Tan, M. Feng, W. Shen, D. Lv and W. Song, Humidity Sensing Using Polymers: A Critical Review of Current Technologies and Emerging Trends, *Chemosensors*, 2024, **12**, 230, DOI: 10.3390/chemosensors12110230.

75 K. Kim, J. Kim, X. Jiang and T. Kim, Static Force Measurement Using Piezoelectric Sensors, *J. Sens.*, 2021, **2021**, DOI: 10.1155/2021/6664200.

76 J. Zhang, X. Wang, X. Chen, X. Xia and G. J. Weng, Piezoelectricity Enhancement in Graphene/Polyvinylidene Fluoride Composites Due to Graphene-Induced α → β Crystal Phase Transition, *Energy Convers. Manage.*, 2022, **269**, 116121, DOI: 10.1016/j.enconman.2022.116121.

77 L. Yang, J. Sun, D. Zhang, H. Bao, R. Zhang, Q. Zhao, Y. Bie, H. He, H. Huang and Y. Xu, A Novel Topographically Patterned MXene@MnO_2/PVDF Piezo-Active Hybrid for Flexible Real-Time and Sensitive Force Sensor, *Compos. Sci. Technol.*, 2023, **241**, 110127, DOI: 10.1016/j.compscitech.2023.110127.

78 M. Li, H. Zang, J. Long, S. Sun and Y. Zhang, Flexible Pressure Sensors Based on Polyvinylidene Fluoride: A Critical Review, *Materials*, 2025, **18**, 615, DOI: 10.3390/ma18030615.

79 I. Aazem, D. T. Mathew, S. Radhakrishnan, K. V. Vijoy, H. John, D. M. Mulvihill and S. C. Pillai, Electrode Materials for Stretchable Triboelectric Nanogenerator in Wearable Electronics, *RSC Adv.*, 2022, **12**, 10545–10572, DOI: 10.1039/D2RA01088G.

80 Z. Shi, Y. Zhang, J. Gu, B. Liu, H. Fu, H. Liang and J. Ji, Triboelectric Nanogenerators: State of the Art, *Sensors*, 2024, **24**, 4298, DOI: 10.3390/s24134298.

81 T. Kamilya, D. Han, J. Shin, S. Kwon and J. Park, An Ultrasensitive Laser-Induced Graphene Electrode-Based Triboelectric Sensor Utilizing Trapped Air as Effective Dielectric Layer, *Polymers*, 2023, **16**, 26, DOI: 10.3390/polym16010026.

82 K.-H. Ha, H. Huh, Z. Li and N. Lu, Soft Capacitive Pressure Sensors: Trends, Challenges, and Perspectives, *ACS Nano*, 2022, **16**, 3442–3448, DOI: 10.1021/acsnano.2c00308.

83 M. Gu, X. Zhou, J. Shen, R. Xie, Y. Su, J. Gao, B. Zhao, J. Li, Y. Duan and Z. Wang, *et al.*, High-Sensitivity, Ultrawide Linear Range, Antibacterial Textile Pressure Sensor Based on Chitosan/MXene Hierarchical Architecture, *iScience*, 2024, **27**, 109481, DOI: 10.1016/j.isci.2024.109481.

84 J. Fu, Z. Deng, C. Liu, C. Liu, J. Luo, J. Wu, S. Peng, L. Song, X. Li and M. Peng, *et al.*, Intelligent, Flexible Artificial Throats with Sound Emitting, Detecting, and Recognizing Abilities, *Sensors*, 2024, **24**, 1493, DOI: 10.3390/s24051493.

85 R. Qin, M. Hu, X. Li, L. Yan, C. Wu, J. Liu, H. Gao, G. Shan and W. Huang, A Highly Sensitive Piezoresistive Sensor Based on MXenes and Polyvinyl Butyral with a Wide Detection Limit and Low Power Consumption, *Nanoscale*, 2020, **12**, 17715–17724, DOI: 10.1039/D0NR02012E.

86 D. P. Pabba, M. Satthiyaraju, A. Ramasdoss, P. Sakthivel, N. Chidhambaram, S. Dhanabalan, C. V. Abarzúa, M. J. Morel, R. Udayabhaskar and R. V. Mangalaraja, *et al.*, MXene-Based Nanocomposites for Piezoelectric and Triboelectric Energy Harvesting Applications, *Micromachines*, 2023, **14**, 1273, DOI: 10.3390/mi14061273.

87 J. Zhang, C. Boyer and Y. X. Zhang, Enhancing the Humidity Resistance of Triboelectric Nanogenerators: A Review, *Small*, 2024, **20**(36), DOI: 10.1002/smll.202401846.

88 O. Cetin, M. O. Cicek, M. Cugunlular, T. Bolukbasi, Y. Khan and H. E. Unalan, MXene-Deposited Melamine Foam-Based Iontronic Pressure Sensors for Wearable Electronics and Smart Numpads, *Small*, 2024, **20**(45), DOI: 10.1002/smll.202403202.

89 C. A. Banciu, F. Nastase, A.-I. Istrate and L. M. Veca, 3D Graphene Foam by Chemical Vapor Deposition: Synthesis, Properties, and Energy-Related Applications, *Molecules*, 2022, **27**, 3634, DOI: 10.3390/molecules27113634.

90 R. Liu, J. Li, M. Li, Q. Zhang, G. Shi, Y. Li, C. Hou and H. Wang, MXene-Coated Air-Permeable Pressure-Sensing Fabric for Smart Wear, *ACS Appl. Mater. Interfaces*, 2020, **12**, 46446–46454, DOI: 10.1021/acsami.0c11715.

91 M. R. Islam, S. Afroj, C. Beach, M. H. Islam, C. Parraman, A. Abdelkader, A. J. Casson, K. S. Novoselov and N. Karim, Fully Printed and Multifunctional Graphene-Based Wearable e-Textiles for Personalized Healthcare

Applications, *iScience*, 2022, **25**, 103945, DOI: 10.1016/j.isci.2022.103945.

92 S. Devinder, S. Joseph, S. Pandey and J. Joseph, Low-Cost, Interdigitated Capacitive Sensor Using Laser-Written Graphene Foam for Touch, Proximity, and Liquid Level Detection, *Appl. Phys. Lett.*, 2023, **123**(16), DOI: 10.1063/5.0178446.

93 S. Mandal, I. Arief, S. Chae, M. Tahir, T. X. Hoang, G. Heinrich, S. Wießner and A. Das, Self-Repairable Hybrid Piezoresistive-Triboelectric Sensor Cum Nanogenerator Utilizing Dual-Dynamic Reversible Network in Mechanically Robust Modified Natural Rubber, *Adv. Sens. Res.*, 2024, **3**(10), DOI: 10.1002/adsr.202400036.

94 H. Liang, L. Zhang, T. Wu, H. Song and C. Tang, Dual-Mode Flexible Sensor Based on PVDF/MXene Nanosheet/Reduced Graphene Oxide Composites for Electronic Skin, *Nanomaterials*, 2022, **13**, 102, DOI: 10.3390/nano13010102.

95 Md. R. Repon, D. Mikučionienė, T. K. Paul, J. Y. Al-Humaidi, M. M. Rahman, T. Islam and S. Shukhratov, Architectural Design and Affecting Factors of MXene-Based Textronics for Real-World Application, *RSC Adv.*, 2024, **14**, 16093–16116, DOI: 10.1039/D4RA01820F.

96 J. Zhou, X. Long, J. Huang, C. Jiang, F. Zhuo, C. Guo, H. Li, Y. Fu and H. Duan, Multiscale and Hierarchical Wrinkle Enhanced Graphene/Ecoflex Sensors Integrated with Human-Machine Interfaces and Cloud-Platform, *npj Flexible Electron.*, 2022, **6**, 55, DOI: 10.1038/s41528-022-00189-1.

97 F. Zhang, K. Yang, Z. Pei, Y. Wu, S. Sang, Q. Zhang and H. Jiao, A Highly Accurate Flexible Sensor System for Human Blood Pressure and Heart Rate Monitoring Based on Graphene/Sponge, *RSC Adv.*, 2022, **12**, 2391–2398, DOI: 10.1039/D1RA08608A.

98 M. I. H. Protyai and A. Bin Rashid, A Comprehensive Overview of Recent Progress in MXene-Based Polymer Composites: Their Fabrication Processes, Advanced Applications, and Prospects, *Heliyon*, 2024, **10**, e37030, DOI: 10.1016/j.heliyon.2024.e37030.

99 H. Yuan, Q. Zhang, T. Zhou, W. Wu, H. Li, Z. Yin, J. Ma and T. Jiao, Progress and Challenges in Flexible Capacitive Pressure Sensors: Microstructure Designs and Applications, *Chem. Eng. J.*, 2024, **485**, 149926, DOI: 10.1016/j.cej.2024.149926.

100 S. Yang, Y.-J. Cao, K. Han, J.-T. Guo, P.-L. Zheng, L.-Y. Wang, T. Cheng, Y.-Z. Zhang and W.-Y. Lai, Stretchable Transparent Electrodes Based on Metal Grid Hybrids for Skin-like Multimodal Sensing and Flexible Touch Panel, *Nano Energy*, 2025, **139**, 110942, DOI: 10.1016/j.nanoen.2025.110942.

101 D. Barmpakos, V. Belessi, N. Xanthopoulos, C. A. Krontiras and G. Kaltsas, Flexible Inkjet-Printed Heaters Utilizing Graphene-Based Inks, *Sensors*, 2022, **22**, 1173, DOI: 10.3390/s22031173.

102 M. Khan, K. Indykiewicz, P. Tam and A. Yurgens, High Mobility Graphene on EVA/PET, *Nanomaterials*, 2022, **12**, 331, DOI: 10.3390/nano12030331.

103 P. Zhao, R. Zhang, Y. Tong, X. Zhao, T. Zhang, X. Wang, Q. Tang and Y. Liu, Shape-Designable and Reconfigurable All-Paper Sensor through the Sandwich Architecture for Pressure/Proximity Detection, *ACS Appl. Mater. Interfaces*, 2021, **13**, 49085–49095, DOI: 10.1021/acsami.1c14523.

104 X. He, X. He, H. He, S. Liang, Z. Liu, J. Liang, Y. Xin, W. Yang, Y. Chen and C. Zhang, Large-Scale, Cuttable, Full Tissue-Based Capacitive Pressure Sensor for the Detection of Human Physiological Signals and Pressure Distribution, *ACS Omega*, 2021, **6**, 27208–27215, DOI: 10.1021/acsomega.1c03900.

105 W. Jia, Q. Zhang, Y. Cheng, J. Wang, H. Zhang, S. Sang and J. Ji, A Flexible Capacitive Paper-Based Pressure Sensor Fabricated Using 3D Printing, *Chemosensors*, 2022, **10**, 432, DOI: 10.3390/chemosensors10100432.

106 T. Akram, B. Zhang and G. Zhao, MXene-Polymer Hydrogel Sensors for Next-Generation Advanced Wearable Sensing: From Synthesis to Real World Integration, *Adv. Mater. Technol.*, 2025, **10**(10), DOI: 10.1002/admt.202500906.

107 T. Peng, R. Wu, B. Wang, T. Liskiewicz and S. Shi, Long-Term Storage of $Ti_3C_2T_x$ Aqueous Dispersion with Stable Electrochemical Properties, *Materials*, 2024, **17**, 5414, DOI: 10.3390/ma17225414.

108 R. Wei, H. Li, Z. Chen, Q. Hua, G. Shen and K. Jiang, Revolutionizing Wearable Technology: Advanced Fabrication Techniques for Body-Conformable Electronics, *npj Flexible Electron.*, 2024, **8**, 83, DOI: 10.1038/s41528-024-00370-8.

109 Z.-D. Zhang, X.-F. Zhao, Q.-C. Zhang, J. Liang, H.-N. Zhang, T.-S. Zhang and C.-Y. Xue, Fully Sprayed MXene-Based High-Performance Flexible Piezoresistive Sensor for Image Recognition, *Nano Mater. Sci.*, 2024, **6**, 77–85, DOI: 10.1016/j.nanoms.2023.06.001.

110 K. Anagnostou, M. Urban, E. Sotiropoulos, C. Polyzoidis, K. Kavalieraki, K. Mouratis, G. Rosati, A. Merkoçi, K. Rogdakis and E. Kymakis, Water-Based Graphene Oxide Inks for Inkjet-Printed Flexible Moisture Energy Generators, *Sci. Rep.*, 2025, **15**, 24685, DOI: 10.1038/s41598-025-09628-1.

111 P. Das, P. K. Marvi, S. Ganguly, X. Tang, B. Wang, S. Srinivasan, A. R. Rajabzadeh and A. Rosenkranz, MXene-Based Elastomer Mimetic Stretchable Sensors: Design, Properties, and Applications, *Nano-Micro Lett.*, 2024, **16**, 135.

112 Y. Shao, L. Wei, X. Wu, C. Jiang, Y. Yao, B. Peng, H. Chen, J. Huangfu, Y. Ying and C. J. Zhang, *et al.*, Room-Temperature High-Precision Printing of Flexible Wireless Electronics Based on MXene Inks, *Nat. Commun.*, 2022, **13**, 3223, DOI: 10.1038/s41467-022-30648-2.

113 P. He, J. Cao, H. Ding, C. Liu, J. Neilson, Z. Li, I. A. Kinloch and B. Derby, Screen-Printing of a Highly Conductive Graphene Ink for Flexible Printed Electronics, *ACS Appl. Mater. Interfaces*, 2019, **11**, 32225–32234, DOI: 10.1021/acsami.9b04589.

114 Z. Wu, S. Liu, Z. Hao and X. Liu, MXene Contact Engineering for Printed Electronics, *Adv. Sci.*, 2023, **10**(19), DOI: 10.1002/advs.202207174.

115 F. C. Rufino, A. M. Pascon, L. C. J. Espindola, F. H. Cioldin, D. R. G. Larrudé and J. A. Diniz, Definition of CVD Graphene Micro Ribbons with Lithography and Oxygen Plasma Ashing, *Carbon Trends*, 2021, **4**, 100056, DOI: 10.1016/j.cartre.2021.100056.

116 S. Bae, H. Kim, Y. Lee, X. Xu, J.-S. Park, Y. Zheng, J. Balakrishnan, T. Lei, H. Ri Kim and Y. Il Song, *et al.*, Roll-to-Roll Production of 30-Inch Graphene Films for Transparent Electrodes, *Nat. Nanotechnol.*, 2010, **5**, 574–578, DOI: 10.1038/nnano.2010.132.

117 X. Zheng, Q. Hu, Z. Wang, W. Nie, P. Wang and C. Li, Roll-to-Roll Layer-by-Layer Assembly Bark-Shaped Carbon Nanotube/$Ti_3C_2T_x$ MXene Textiles for Wearable Electronics, *J. Colloid Interface Sci.*, 2021, **602**, 680–688, DOI: 10.1016/j.jcis.2021.06.043.

118 A. M. Amani, L. Tayebi, M. Abbasi, A. Vaez, H. Kamyab, S. Chelliapan and E. Vafa, The Need for Smart Materials in an Expanding Smart World: MXene-Based Wearable Electronics and Their Advantageous Applications, *ACS Omega*, 2023, **9**(3), 3123–3142, DOI: 10.1021/acsomega.3c06590.

119 A. Iqbal, J. Hong, T. Y. Ko and C. M. Koo, Improving Oxidation Stability of 2D MXenes: Synthesis, Storage Media, and Conditions, *Nano Convergence*, 2021, **8**, 9, DOI: 10.1186/s40580-021-00259-6.

120 W. Lu, B. Mustafa, Z. Wang, F. Lian and G. Yu, PDMS-Encapsulated MXene@Polyester Fabric Strain Sensor for Multifunctional Sensing Applications, *Nanomaterials*, 2022, **12**, 871, DOI: 10.3390/nano12050871.

121 D. Kireev, J. Kampfe, A. Hall and D. Akinwande, Graphene Electronic Tattoos 2.0 with Enhanced Performance, Breathability and Robustness, *npj 2D Mater. Appl.*, 2022, **6**, 46, DOI: 10.1038/s41699-022-00324-6.

122 M. Liu, L. Zheng, K. Zha, Y. Yang, Y. Hu, K. Chen, F. Wang, K. Zhang, W. Liu and B. Mi, *et al.*, Cu(II)@MXene Based Photothermal Hydrogel with Antioxidative and Antibacterial Properties for the Infected Wounds, *Front. Bioeng. Biotechnol.*, 2023, **13**, DOI: 10.3389/fbioe.2023.1308184.

123 H. Jang, K. Sel, E. Kim, S. Kim, X. Yang, S. Kang, K.-H. Ha, R. Wang, Y. Rao and R. Jafari, *et al.*, Graphene E-Tattoos for Unobstructive Ambulatory Electrodermal Activity Sensing on the Palm Enabled by Heterogeneous Serpentine Ribbons, *Nat. Commun.*, 2022, **13**, 6604, DOI: 10.1038/s41467-022-34406-2.

124 L. Liu, L. Wang, X. Liu, W. Yuan, M. Yuan, Q. Xia, Q. Hu and A. Zhou, High-Performance Wearable Strain Sensor Based on MXene@Cotton Fabric with Network Structure, *Nanomaterials*, 2021, **11**, 889, DOI: 10.3390/nano11040889.

125 Y. Ma, K. Zhao, J. Han, B. Han, M. Wang, Z. Tong, J. Suhr, L. Xiao, S. Jia and X. Chen, Pressure Sensor Based on a Lumpily Pyramidal Vertical Graphene Film with a Broad Sensing Range and High Sensitivity, *ACS Appl. Mater. Interfaces*, 2023, **15**, 13813–13821, DOI: 10.1021/acsami.3c01175.

126 Y. Wang, Z. Qin, D. Wang, D. Liu, Z. Wang, A. Jazzar, P. He, Z. Guo, X. Chen and C. Jia, *et al.*, Microstructure-Reconfigured Graphene Oxide Aerogel Metamaterials for Ultrarobust Directional Sensing at Human–Machine Interfaces, *Nano Lett.*, 2024, **24**, 12000–12009, DOI: 10.1021/acs.nanolett.4c03706.

127 M. Ren, Z. Sun, M. Zhang, X. Yang, D. Guo, S. Dong, R. Dhakal, Z. Yao, Y. Li and N. Y. Kim, A High-Performance Wearable Pressure Sensor Based on an MXene/PVP Composite Nanofiber Membrane for Health Monitoring, *Nanoscale Adv.*, 2022, **4**, 3987–3995, DOI: 10.1039/D2NA00339B.

128 S. K. Ghosh, J. Kim, M. P. Kim, S. Na, J. Cho, J. J. Kim and H. Ko, Ferroelectricity-Coupled 2D-MXene-Based Hierarchically Designed High-Performance Stretchable Triboelectric Nanogenerator, *ACS Nano*, 2022, **16**, 11415–11427, DOI: 10.1021/acsnano.2c05531.

129 S. Wang, H.-Q. Shao, Y. Liu, C.-Y. Tang, X. Zhao, K. Ke, R.-Y. Bao, M.-B. Yang and W. Yang, Boosting Piezoelectric Response of PVDF-TrFE via MXene for Self-Powered Linear Pressure Sensor, *Compos. Sci. Technol.*, 2021, **202**, 108600, DOI: 10.1016/j.compscitech.2020.108600.

130 A. Ahmed, N. A. Khoso, M. F. Arain, I. A. Khan, K. Javed, A. Khan, S. I. Memon, Q. Fan and J. Shao, Development of Highly Flexible Piezoelectric PVDF-TRFE/Reduced Graphene Oxide Doped Electrospun Nano-Fibers for Self-Powered Pressure Sensor, *Polymers*, 2024, **16**(13), DOI: 10.3390/polym16131781.

131 L. A. Kurup, C. M. Cole, J. N. Arthur and S. D. Yambem, Graphene Porous Foams for Capacitive Pressure Sensing, *ACS Appl. Nano Mater.*, 2022, **5**, 2973–2983, DOI: 10.1021/acsanm.2c00247.

132 E. Keel, A. Ejaz, M. Mckinlay, M. P. Garcia, M. Caffio, D. Gibson and C. García Núñez, Three-Dimensional Graphene Foam Based Triboelectric Nanogenerators for Energy Systems and Autonomous Sensors, *Nano Energy*, 2023, **112**, 108475, DOI: 10.1016/j.nanoen.2023.108475.

133 S. Sharma, A. Chhetry, M. Sharifuzzaman, H. Yoon and J. Y. Park, Wearable Capacitive Pressure Sensor Based on MXene Composite Nanofibrous Scaffolds for Reliable Human Physiological Signal Acquisition, *ACS Appl. Mater. Interfaces*, 2020, **12**, 22212–22224, DOI: 10.1021/acsami.0c05819.

134 L. Zhang, J. Pang, X. Lu, X. Zhang and X. Zhang, Wearable Flexible Wireless Pressure Sensor Based on Poly(Vinyl Alcohol)/Carbon Nanotube/MXene Composite for Health Monitoring, *Micromachines*, 2025, **16**, 1132, DOI: 10.3390/mi16101132.

135 Y. Xiao, Q. Pu, C. Wang, X. Jia, S. Sun, Q. Jin, X. Wang, B. Wang, P. Sun and F. Liu, *et al.*, Wearable Self-Powered Pressure Sensors Based on alk-$Ti_3C_2T_x$ Regulating Contact Barrier Difference for Noncontact Motion Object Recognition, *Adv. Sci.*, 2025, **12**(13), DOI: 10.1002/advs.202416504.

136 L. Zhang, J. Pang, X. Lu, X. Zhang and X. Zhang, Wearable Flexible Wireless Pressure Sensor Based on Poly(Vinyl Alcohol)/Carbon Nanotube/MXene Composite for Health Monitoring, *Micromachines*, 2025, **16**, 1132, DOI: 10.3390/mi16101132.

137 H.-S. Jang, K. H. Lee and B. H. Kim, Flexible Mechanical Sensors Fabricated with Graphene Oxide-Coated Commercial Silk, *Nanomaterials*, 2024, **14**, 1000, DOI: 10.3390/nano14121000.

138 P. Miao, J. Wang, C. Zhang, M. Sun, S. Cheng and H. Liu, Graphene Nanostructure-Based Tactile Sensors for Electronic Skin Applications, *Nano-Micro Lett.*, 2019, **11**, 71, DOI: 10.1007/s40820-019-0302-0.

139 F. Niu, Z. Qin, L. Min, B. Zhao, Y. Lv, X. Fang and K. Pan, Ultralight and Hyperelastic Nanofiber-Reinforced MXene–Graphene Aerogel for High-Performance Piezoresistive Sensor, *Adv. Mater. Technol.*, 2021, **6**(11), DOI: 10.1002/admt.202100394.

140 L. Bi, Z. Yang, L. Chen, Z. Wu and C. Ye, Compressible AgNWs/$Ti_3C_2T_x$ MXene Aerogel-Based Highly Sensitive Piezoresistive Pressure Sensor as Versatile Electronic Skins, *J. Mater. Chem. A*, 2020, **8**, 20030–20036, DOI: 10.1039/D0TA07044K.

141 A. Wang, Z. Gao, S. Wu, Y. Wei, B. Lu, J. Shi, L. Shen, Y. Liu, X. Sun and Z. Wen, Superelastic and Ultra-Soft MXene/CNF Aerogel@PDMS-Based Dual-Modal Pressure Sensor for Complex Stimuli Monitoring, *Adv. Sci.*, 2025, **12**(26), DOI: 10.1002/advs.202502797.

142 M. Zhu, Y. Yue, Y. Cheng, Y. Zhang, J. Su, F. Long, X. Jiang, Y. Ma and Y. Gao, Hollow MXene Sphere/Reduced Graphene Aerogel Composites for Piezoresistive Sensor with Ultra-High Sensitivity, *Adv. Electron. Mater.*, 2020, **6**(2), DOI: 10.1002/aelm.201901064.

143 W. Li, J. Zhou, W. Sheng, Y. Jia, W. Xu and T. Zhang, Highly Flexible and Compressible 3D Interconnected Graphene Foam for Sensitive Pressure Detection, *Micromachines*, 2024, **15**, 1355, DOI: 10.3390/mi15111355.

144 S. Tian, L. Wang and R. Zhu, A Flexible Multimodal Pulse Sensor for Wearable Continuous Blood Pressure Monitoring, *Mater. Horiz.*, 2024, **11**, 2428–2437, DOI: 10.1039/D3MH01999C.

145 R. R. Kisannagar, J. Lee, Y. Park and I. Jung, Development of a PVDF/1D–2D Nanofiller Porous Structure Pressure Sensor Using near-Field Electrospinning for Human Motion and Vibration Sensing, *J. Mater. Chem. C*, 2025, **13**, 5700–5710, DOI: 10.1039/D4TC05253F.

146 R. Xu, D. Wang, H. Zhang, N. Xie, S. Lu and K. Qu, Simultaneous Detection of Static and Dynamic Signals by a Flexible Sensor Based on 3D Graphene, *Sensors*, 2017, **17**, 1069, DOI: 10.3390/s17051069.

147 X. Shi, X. Fan, Y. Zhu, Y. Liu, P. Wu, R. Jiang, B. Wu, H.-A. Wu, H. Zheng and J. Wang, *et al.*, Pushing Detectability and Sensitivity for Subtle Force to New Limits with Shrinkable Nanochannel Structured Aerogel, *Nat. Commun.*, 2022, **13**, 1119, DOI: 10.1038/s41467-022-28760-4.

148 S. Kumar, S. M. Zain Mehdi, M. Taunk, S. Kumar, A. Aherwar, S. Singh and T. Singh, Synergistic Effects of Polymer Integration on the Properties, Stability, and Applications of MXenes, *J. Mater. Chem. A*, 2025, **13**, 11050–11113, DOI: 10.1039/D4TA08094G.

149 C. Liu, F. Ma, Q. Sun, Q. Hu, W. Tong, X. Guo, R. Hu, P. Liu, Y. Huang and X. Hao, *et al.*, Highly Sensitive Flexible Capacitive Pressure Sensor Based on a Multicross-Linked Dual-Network Ionic Hydrogel for Blood Pressure Monitoring Applications, *ACS Appl. Mater. Interfaces*, 2024, **16**, 34042–34056, DOI: 10.1021/acsami.4c04686.

150 Y. Wang, T. Guo, Z. Tian, L. Shi, S. C. Barman and H. N. Alshareef, MXenes for Soft Robotics, *Matter*, 2023, **6**, 2807–2833.

151 C. Qu, M. Lu, Z. Zhang, S. Chen, D. Liu, D. Zhang, J. Wang and B. Sheng, Flexible Microstructured Capacitive Pressure Sensors Using Laser Engraving and Graphitization from Natural Wood, *Molecules*, 2023, **28**, 5339, DOI: 10.3390/molecules28145339.

152 Y. Peng, J. Zhou, X. Song, K. Pang, A. Samy, Z. Hao and J. Wang, A Flexible Pressure Sensor with Ink Printed Porous Graphene for Continuous Cardiovascular Status Monitoring, *Sensors*, 2021, **21**, 485, DOI: 10.3390/s21020485.

153 B. Osuagwu, E. McCaughey and M. Purcell, A Pressure Monitoring Approach for Pressure Ulcer Prevention, *BMC Biomed. Eng.*, 2023, **5**, 8, DOI: 10.1186/s42490-023-00074-6.

154 Y. Yoo and B.-D. Choi, Readout Circuits for Capacitive Sensors, *Micromachines*, 2021, **12**, 960, DOI: 10.3390/mi12080960.

155 S. Szunerits, T. Rodrigues, R. Bagale, H. Happy, R. Boukherroub and W. Knoll, Graphene-Based Field-Effect Transistors for Biosensing: Where Is the Field Heading To?, *Anal. Bioanal. Chem.*, 2024, **416**, 2137–2150, DOI: 10.1007/s00216-023-04760-1.

156 Y. Zi, S. Niu, J. Wang, Z. Wen, W. Tang and Z. L. Wang, Standards and Figure-of-Merits for Quantifying the Performance of Triboelectric Nanogenerators, *Nat. Commun.*, 2015, **6**, 8376, DOI: 10.1038/ncomms9376.

157 A. H. Anwer, N. Khan, M. Z. Ansari, S.-S. Baek, H. Yi, S. Kim, S. M. Noh and C. Jeong, Recent Advances in Touch Sensors for Flexible Wearable Devices, *Sensors*, 2022, **22**, 4460, DOI: 10.3390/s22124460.

158 R. Zhang and H. Olin, Advances in Inorganic Nanomaterials for Triboelectric Nanogenerators, *ACS Nanosci. Au*, 2022, **2**, 12–31, DOI: 10.1021/acsnanoscienceau.1c00026.

159 M. G. Stanford, J. T. Li, Y. Chyan, Z. Wang, W. Wang and J. M. Tour, Laser-Induced Graphene Triboelectric Nanogenerators, *ACS Nano*, 2019, **13**, 7166–7174, DOI: 10.1021/acsnano.9b02596.

160 J. Fan, M. Yuan, L. Wang, Q. Xia, H. Zheng and A. Zhou, MXene Supported by Cotton Fabric as Electrode Layer of Triboelectric Nanogenerators for Flexible Sensors, *Nano Energy*, 2023, **105**, 107973, DOI: 10.1016/j.nanoen.2022.107973.

161 Y. Chen, X. Gong and J. Gai, Progress and Challenges in Transfer of Large-Area Graphene Films, *Adv. Sci.*, 2016, **3**(8), DOI: 10.1002/advs.201500343.

162 W. Yang, F. Liu, Y. Lin, J. Wang, C. Zhang, H. Cheng and H. Chen, MXene-Based Flexible Sensors for Wearable Applications, *Soft Sci.*, 2025, **5**(33), DOI: 10.20517/ss.2025.12.

163 X. Qi, J. Luo, H. Liu, S. Fan, Z. Ren, P. Wang, S. Yu and J. Wei, Flexible Strain Sensors Based on Printing Technology: Conductive Inks, Substrates, Printability, and Applications, *Materials*, 2025, **18**, 2113, DOI: 10.3390/ma18092113.

164 A. DeHennis and J. Chae, Pressure Sensors, in *Comprehensive Microsystems*, Elsevier, 2008, pp. 101–133.

165 C. Fang, T. Tong, T. Bu, Y. Cao, S. Xu, Y. Qi and C. Zhang, Overview of Power Management for Triboelectric Nanogenerators, *Adv. Intell. Syst.*, 2020, **2**(2), DOI: 10.1002/aisy.201900129.

166 D. Kim, A. Chhetry, M. A. Zahed, S. Sharma, S. Jeong, H. Song and J. Y. Park, Highly Sensitive and Reliable Piezoresistive Strain Sensor Based on Cobalt Nanoporous Carbon-Incorporated Laser-Induced Graphene for Smart Healthcare Wearables, *ACS Appl. Mater. Interfaces*, 2023, **15**, 1475–1485, DOI: 10.1021/acsami.2c15500.

167 H. R. Na, H. J. Lee, J. H. Jeon, H.-J. Kim, S.-K. Jerng, S. B. Roy, S.-H. Chun, S. Lee and Y. J. Yun, Vertical Graphene on Flexible Substrate, Overcoming Limits of Crack-Based Resistive Strain Sensors, *npj Flexible Electron.*, 2022, **6**, 2, DOI: 10.1038/s41528-022-00135-1.

168 Y. Yin, C. Guo, H. Li, H. Yang, F. Xiong and D. Chen, The Progress of Research into Flexible Sensors in the Field of Smart Wearables, *Sensors*, 2022, **22**, 5089, DOI: 10.3390/s22145089.

169 G. Yang, Y. Li, J. Zhu, L. Ma, Z. Li, J. Wang and S. Yang, Highly Robust, Processable and Multi-Functional PDMS/Graphene Composite Aerogel Constructed by "Soft-Hard" Interface Engineering Strategy, *Composites, Part B*, 2025, **288**, 111904, DOI: 10.1016/j.compositesb.2024.111904.

170 F.-L. Gao, J. Liu, X.-P. Li, Q. Ma, T. Zhang, Z.-Z. Yu, J. Shang, R.-W. Li and X. Li, $Ti_3C_2T_x$ MXene-Based Multifunctional Tactile Sensors for Precisely Detecting and Distinguishing Temperature and Pressure Stimuli, *ACS Nano*, 2023, **17**, 16036–16047, DOI: 10.1021/acsnano.3c04650.

171 H. Liu, C. Du, L. Liao, H. Zhang, H. Zhou, W. Zhou, T. Ren, Z. Sun, Y. Lu and Z. Nie, *et al.*, Approaching Intrinsic Dynamics of MXenes Hybrid Hydrogel for 3D Printed Multimodal Intelligent Devices with Ultrahigh Superelasticity and Temperature Sensitivity, *Nat. Commun.*, 2022, **13**, 3420, DOI: 10.1038/s41467-022-31051-7.

172 C. G. Núñez, W. T. Navaraj, E. O. Polat and R. Dahiya, Energy-Autonomous, Flexible, and Transparent Tactile Skin, *Adv. Funct. Mater.*, 2017, **27**(18), DOI: 10.1002/adfm.201606287.